

Structure–Affinity Relationships of 2,3,4,5-Tetrahydro-1*H*-3-benzazepine and 6,7,8,9-Tetrahydro-5*H*-benzo[7]annulen-7-amine Analogues and the Discovery of a Radiofluorinated 2,3,4,5-Tetrahydro-1*H*-3-benzazepine Congener for Imaging GluN2B Subunit-Containing *N*-Methyl-D-aspartate Receptors

Hazem Ahmed,^{†,||} Ahmed Haider,^{†,||} Jasmine Varisco,[†] Maja Stanković,[†] Rahel Wallimann,[†] Stefan Gruber,[†] Irina Iten,[†] Surya Häne,[†] Adrienne Müller Herde,[†] Claudia Keller,[†] Roger Schibli,^{†,‡} Dirk Schepmann,[§] Linjing Mu,^{†,‡} Bernhard Wünsch,[§] and Simon M. Ametamey^{*,†,||}

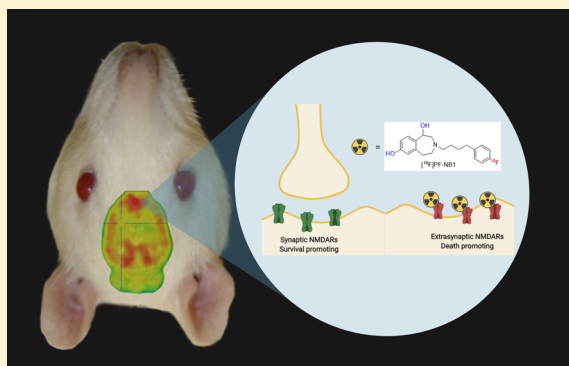
[†]Institute of Pharmaceutical Sciences, ETH Zurich, Vladimir-Prelog-Weg 4, 8093 Zurich, Switzerland

[‡]Department of Nuclear Medicine, University Hospital Zurich, 8091 Zurich, Switzerland

[§]Institute of Pharmaceutical and Medicinal Chemistry, University of Münster, Corrensstr. 48, 48149 Münster, Germany

S Supporting Information

ABSTRACT: Aspiring to develop a positron emission tomography (PET) imaging agent for the GluN2B subunits of the *N*-methyl-D-aspartate receptor (NMDAR), a key therapeutic target for drug development toward several neurological disorders, we synthesized a series of 2,3,4,5-tetrahydro-1*H*-3-benzazepine and 6,7,8,9-tetrahydro-5*H*-benzo[7]annulen-7-amine analogues. After in vitro testing via competition binding assay and autoradiography, [¹⁸F]PF-NB1 emerged as the best performing tracer with respect to specificity and selectivity over $\sigma 1$ and $\sigma 2$ receptors and was thus selected for further in vivo evaluation. Copper-mediated radiofluorination was accomplished in good radiochemical yields and high molar activities. Extensive in vivo characterization was performed in Wistar rats comprising PET imaging, biodistribution, receptor occupancy, and metabolites studies. [¹⁸F]PF-NB1 binding was selective to GluN2B-rich forebrain regions and was specifically blocked by the GluN2B antagonist, CP-101,606, in a dose-dependent manner with no brain radiometabolites. [¹⁸F]PF-NB1 is a promising fluorine-18 PET tracer for imaging the GluN2B subunits of the NMDAR and has utility for receptor occupancy studies.



INTRODUCTION

L-glutamate is the main excitatory neurotransmitter in the central nervous system (CNS). Glutamatergic receptors can be generally grouped into two classes: ionotropic (iGluRs) receptors (further subdivided into three subtypes: *N*-methyl-D-aspartate receptors (NMDARs), kainate receptors, and 2-amino-3-(3-hydroxy-5-methyl-isoxazol-4-yl)propanoic acid receptors) and metabotropic (mGluRs) receptors (further subdivided into 3 groups: groups I, II, and III).¹ NMDARs are heterotetrameric transmembrane proteins that can bear three different types of subunits: GluN1 subunit (eight splice variants, GluN1a–h), GluN2 subunit (four different genes, GluN2A–D), and GluN3 subunit (two different genes, GluN3A–B). Functional NMDARs typically require the binding of coagonist glycine and agonist glutamate to GluN1 and GluN2 subunits, respectively. Upon activation, the membrane is depolarized, prompting the influx of calcium ions and the propagation of the signals across the synapses.² NMDARs play a fundamental role in neuronal development,

especially neural plasticity as well as learning and memory.^{3–5} In several neuropathological conditions, whether acute or chronic, an elevation of the glutamate synaptic concentration levels can transform glutamate from a vital neurotransmitter for survival to a dangerous neurotoxin, triggering an apoptotic cascade.^{6,7} This neurotoxic process has been found to be associated with several CNS disorders such as Alzheimer's disease, vascular dementia, Parkinson's disease, depression, stroke, and schizophrenia.^{8–10} Numerous drugs have been developed as ion channel blockers; however, they exhibited severe side effects due to hampering of physiological neuronal functions and off-target binding.¹¹ Consequently, subunit-targeting antagonists—more specifically, GluN2B antagonists—have recently emerged as potential therapeutic agents for Parkinson's disease, cerebral ischemia, neuropathic pain, and depression in preclinical assessments.^{12–18} These selective

Received: May 26, 2019

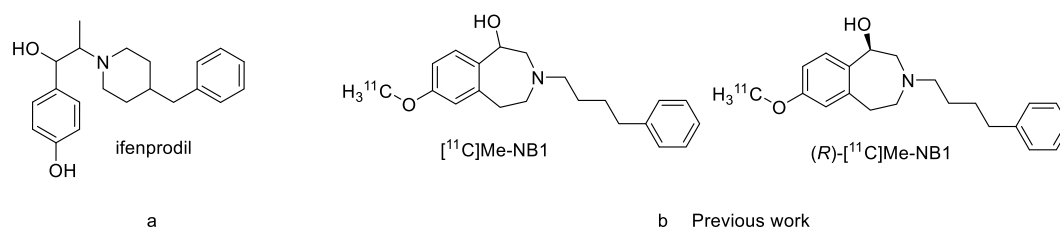


Figure 1. Structures of ifenprodil (a) and (b) of our previously reported $[^{11}\text{C}]$ Me-NB1 and (R)- $[^{11}\text{C}]$ Me-NB1 radiotracers as conformationally restricted analogues of ifenprodil.^{31–33}

GluN2B antagonists possess a better safety profile when compared with the ion channel blockers. This is mainly due to less cerebellum-related side effects such as cognitive and motor effects due to the poor expression of the GluN2B subunit in the cerebellum.^{19,20} The binding site of these antagonists is situated at the interface of the N-terminal domains of GluN1 and GluN2B subunits. This unique binding site was termed the “ifenprodil binding site” after ifenprodil (Figure 1a)—a sigma-1 receptor ($\sigma 1\text{R}$) antagonist—was found to inhibit NMDARs bearing the GluN2B subunit in the 90's.²¹ While the GluN1 subunit shows homogenous expression across the brain, the GluN2B pattern of expression is heterogeneous depending on both the brain's maturity and age.⁵ Although ifenprodil is nonselective and metabolically unstable, it served as a lead compound for the next generation of GluN2B antagonists and as a model for deducing the binding mode and pocket for such ligands from the crystal structure of the GluN1 and GluN2B dimers complexed with ifenprodil (PDB code 3QEL).^{22,23} The forefront challenge facing GluN2B ligands is the off-target binding, especially the $\sigma 1\text{R}$, a distinctive ligand-regulated molecular chaperone in the endoplasmic reticulum that regulates the activity of NMDARs.^{24,25} Nevertheless, several promising and more selective GluN2B antagonists such as CP-101,606 and CERC-303 (MK-0657) have been developed and evaluated in clinical trials.^{12,26} Contrary to the high expectations of these drugs, several clinical trials showed no significant benefit as of yet in patients.^{27,28}

Positron emission tomography (PET) is a noninvasive imaging modality that can functionally assess biological targets using probes with appropriate affinity and selectivity, labeled with positron-emitting radionuclides. For the development of GluN2B therapeutic agents, it can be a pivotal tool to address two essential questions: (1) Does the drug engage GluN2B subunit-containing NMDARs in vivo? (2) If yes, what is the required dose that can show a satisfactory pharmacological response and what is the receptor occupancy for such a response?²⁹ Additionally, side effects can be minimized when PET imaging receptor occupancy studies are employed.³⁰

So far, reported GluN2B subunit imaging probes have suffered from four major drawbacks: brain radiometabolites, substantial off-target binding, low brain uptake, and brain binding patterns inconsistent with reported GluN2B expression patterns.³⁴ While no clinically validated GluN2B PET radiotracer exists, our group recently succeeded in developing the (R)-enantiomer of $[^{11}\text{C}]$ Me-NB1 (K_i (GluN2B) = 5.4 nM, K_i ($\sigma 1$) = 182 nM, K_i ($\sigma 2$) = 554 nM), a 2,3,4,5-tetrahydro-1H-3-benzazepin-1-ol GluN2B PET radiotracer (Figure 1b) that lacks the aforementioned limitations.³¹ Although we demonstrated a successful receptor occupancy (RO) study using $[^{11}\text{C}]$ Me-NB1 with therapeutic GluN2B antagonists, the major inherent limitation of $[^{11}\text{C}]$ Me-NB1 is the short physical half-life of carbon-11 (physical half-life = 20.3 min), which

precludes its transport to imaging centers without an onsite cyclotron. As such, our efforts are currently focused on the development of a fluorine-18 (physical half-life = 109.8 min) labeled GluN2B subunit tracer, where fluorine-18 offers better spatial resolution than carbon-11 and allows distribution of the tracer to nearby PET centers/hospitals (satellite distribution).³⁵ Our preliminary attempts led to (R)- $[^{18}\text{F}]$ OF-Me-NB1, a fluorine-18 analogue of Me-NB1.³⁶ In the course of that work, it came to light that the (R)-enantiomers of 2,3,4,5-tetrahydro-1H-3-benzazepin-1-ols possess a prominent selectivity toward the GluN2B subunit, which was confirmed in a study with the enantiomers of Me-NB1³¹ and other 2,3,4,5-tetrahydro-1H-3-benzazepin-1-ol-based analogues.³⁷ Despite encouraging preclinical findings observed with (R)- $[^{18}\text{F}]$ OF-Me-NB1, the radiofluorinated probe exhibited a relatively fast washout from the brain, thus limiting its utility for GluN2B-specific brain imaging.

In the current study, we report the structure–affinity relationship of a series of derivatives of 2,3,4,5-tetrahydro-1H-3-benzazepines and its closely related structural class of compounds, namely, 6,7,8,9-tetrahydro-5H-benzo[7]annulen-7-amines, that emerged as potential GluN2B antagonists.³⁸ We sought to explore the 6,7,8,9-tetrahydro-5H-benzo[7]annulen-7-amines as potential PET tracers and anticipated that it could be an escape route to the enantiomerically pure restrictions posed by the 2,3,4,5-tetrahydro-1H-3-benzazepine derivatives that we have investigated so far. Rigorous investigation of ifenprodil-like allosteric ligands resulted in a robust pharmacophore model comprising three essential cornerstones: (1) a secondary or tertiary basic amine that is protonated under physiological conditions, (2) a substituted aromatic ring with an electron-donating functionality, and (3) a second aromatic ring, whether substituted or not.³⁹ From these investigations, racemic 14 (PF-NB1) and compound 27 emerged as the best performing compounds considering their GluN2B binding affinity and selectivity over $\sigma 1\text{Rs}$. Surprisingly, even though compound 27 exhibited high nanomolar affinity of 2.1 nM and a reasonable 50-fold selectivity over $\sigma 1\text{R}$, autoradiographic evaluation of $[^{18}\text{F}]$ 27 revealed a homogenous distribution pattern in the rat brain. For compound $[^{18}\text{F}]$ 14 ($[^{18}\text{F}]$ PF-NB1) and its enantiomers, (R)- $[^{18}\text{F}]$ 14 ((R)- $[^{18}\text{F}]$ PF-NB1) and (S)- $[^{18}\text{F}]$ 14 ((S)- $[^{18}\text{F}]$ PF-NB1), we observed a heterogeneous binding distribution that was in accordance with the known expression pattern of GluN2B.³ Although (R)- $[^{18}\text{F}]$ PF-NB1 exhibited a slightly higher in vitro binding affinity, the remarkable autoradiograms with $[^{18}\text{F}]$ PF-NB1 prompted us to select this radioligand for further in vivo evaluation using PET imaging, biodistribution, receptor occupancy, and metabolite studies in rodents.

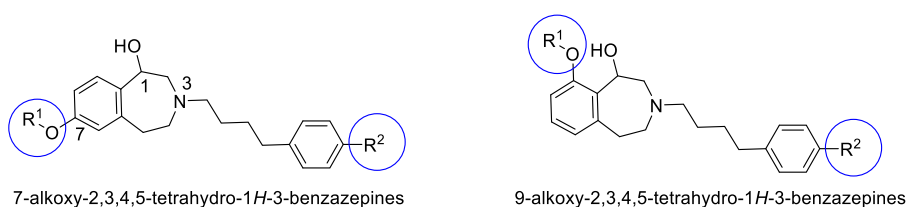
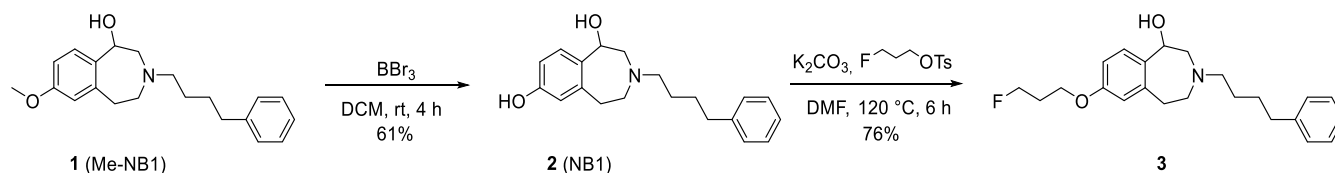
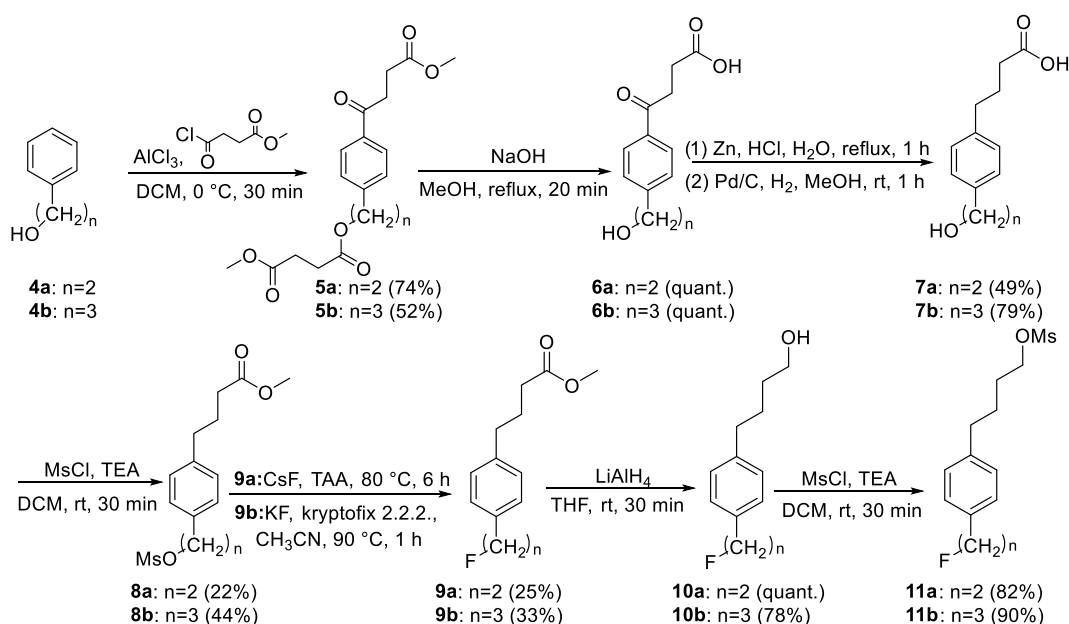


Figure 2. Modification sites pursued for 7- and 9-alkoxy-2,3,4,5-tetrahydro-1H-3-benzazepine derivatives are indicated with substituents R^1 – R^2 .

Scheme 1. Synthesis of Reference Compound 3



Scheme 2. Synthesis of Linkers 11a and 11b



RESULTS AND DISCUSSION

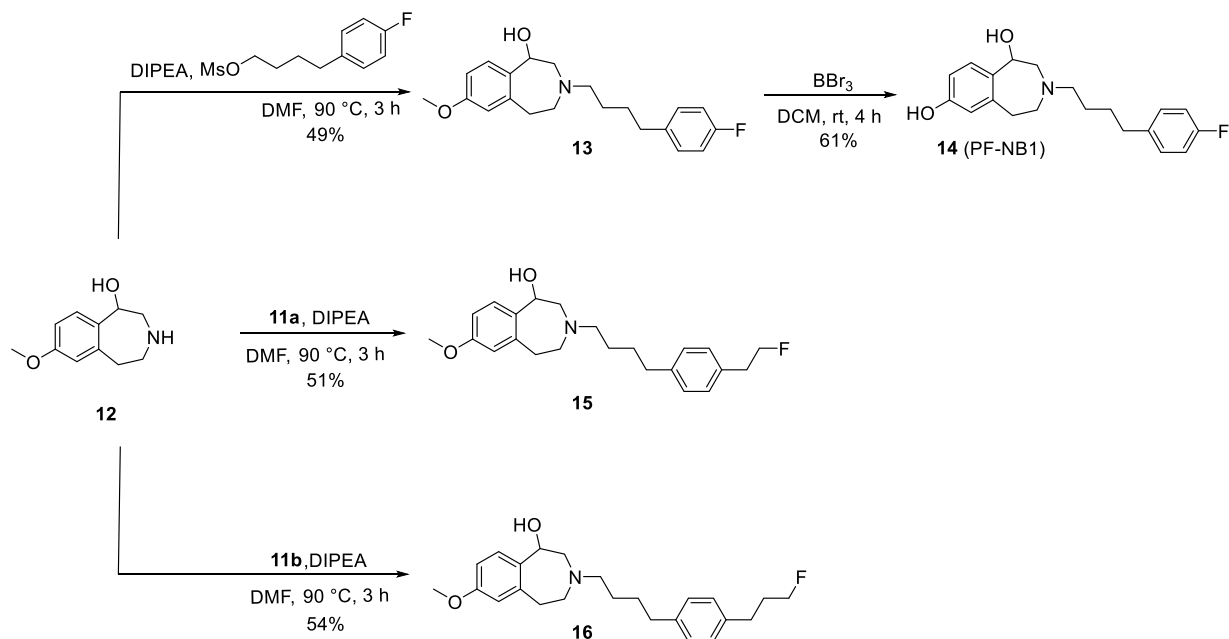
Chemistry. *2,3,4,5-Tetrahydro-1H-3-benzazepines.* For the 2,3,4,5-tetrahydro-1H-3-benzazepin-1-ol scaffold, it has been shown that the benzylic alcohol is crucial for binding to the GluN2B subunit as it exhibits a direct polar interaction with serine 132 of the GluN1 subunit; consequently, we did not pursue any modifications at this structural moiety.^{23,40} Similarly, the length of the alkyl chain was not modified as it was previously shown that a 4-carbon chain length provides an optimal distance between the central amino moiety and the terminal phenyl ring;³² hence, further modifications were envisioned either at the 7-methoxy functionality or on the phenyl ring (Figure 2). All modifications of the phenyl ring were exclusively carried out at the para-position. Furthermore, we investigated shifting the methoxy group from the 7-position to the 9-position.

Demethylation of previously synthesized Me-NB1 by our group³³ was accomplished using BBr_3 to afford phenol 2 in 61% yield (Scheme 1). Late-stage demethylation circumvented the need to undertake additional protection and deprotection steps of the phenolic hydroxyl group described in the original

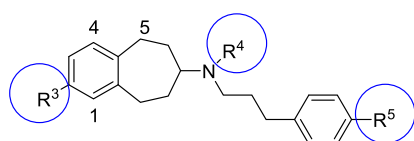
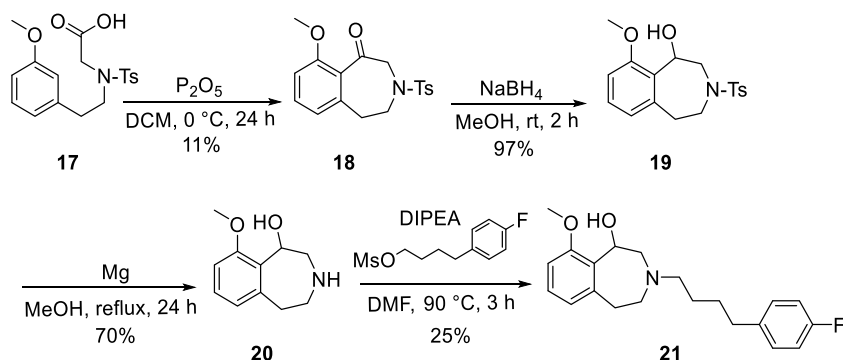
synthesis of phenol 2.⁴¹ O-alkylation of 2 afforded fluoropropyl ether 3 in 76% yield.

The fluorinated mesylates, 11a and 11b, were synthesized as shown in Scheme 2 applying a nine-step synthetic approach under the same conditions and in similar yields. With the aim to introduce steric hindrance, alcohols 4a and 4b were protected with a bulky methyl succinate ester moiety, thereby favoring subsequent para-directed Friedel–Crafts acylation. This strategy afforded keto acids 5a and 5b in 74 and 52% yields, respectively. Cleavage of the ester functionalities in 5a and 5b was achieved by treatment with sodium hydroxide under reflux to afford alcohols 6a and 6b in quantitative yields. Reduction of ketones 6a and 6b under modified Clemmensen conditions⁴² with zinc and concentrated HCl yielded an inseparable mixture of phenylbutanoic and phenylbutenoic acid products in a ratio of 1:4. The mixture was subjected to palladium-catalyzed hydrogenation to yield intermediates 7a and 7b exclusively in overall yields of 49 and 79%, respectively. The free alcohols were mesylated using mesyl chloride; interestingly, we observed an unexpected simultaneous methylation of the carboxylic acid, yielding methyl esters 8a

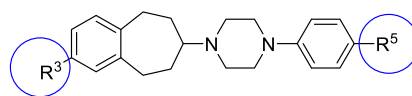
Scheme 3. Synthesis of Reference Compounds 14, 15, and 16 with a Methoxy Moiety in 7-Position



Scheme 4. Synthesis of Reference Compound 21 with a 9-Methoxy Moiety



Alkyl 6,7,8,9-tetrahydro-5H-benzo[7]annulene derivatives



Piperazine 6,7,8,9-tetrahydro-5H-benzo[7]annulene derivatives

Figure 3. Alkylamino and piperazinyl substituted 6,7,8,9-tetrahydro-5H-benzo[7]annulene derivatives with possible sites of modifications indicated with R^3 – R^5 .

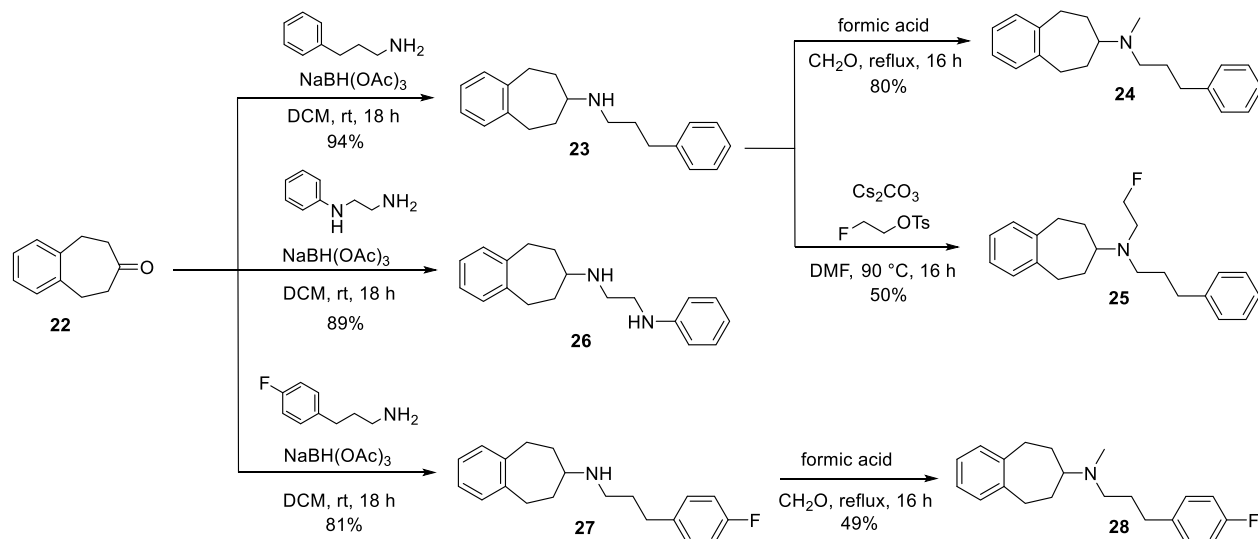
and **8b**.⁴³ Fluorination of **8a** by using the KF/kryptofix 2.2.2 system did not yield the desired fluorinated product; however, using CsF as a fluorinating agent in *tert*-amyl alcohol afforded intermediate **9a** in 25% yield. Compound **9b**, on the other hand, was obtained using KF/kryptofix 2.2.2 in a higher yield of 33%. Subsequent reduction of the ester afforded fluorinated alcohols **10a** and **10b** in quantitative and 78% yields, respectively. In the final step, alcohols **10a** and **10b** were mesylated to afford **11a** and **11b** in 82 and 90% yields, respectively.

N-alkylation of the commercially available key intermediate **12** with custom synthesized [4-(4-fluorophenyl)butyl] methanesulfonate⁴⁴ afforded intermediate **13** in 49% yield. Further treatment with BBr_3 yielded phenolic reference compound **14**

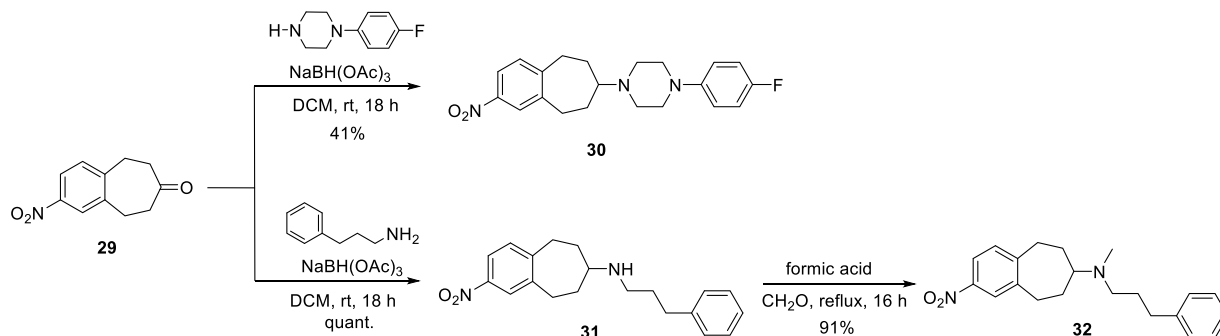
(PF-NB1) in 61% yield. Separation of the enantiomers by chiral high-performance liquid chromatography (HPLC) yielded the two enantiomers, (*S*)-**14** and (*R*)-**14**. The circular dichroism (CD) spectra for both enantiomers were recorded and compared to the enantiomers of Me-NB1, to which we previously determined the absolute configuration by means of X-ray crystallography (Supporting Information, Figure 1).³¹ Key intermediate **12** was reacted with the mesylates, **11a** and **11b**, to afford reference compounds **15** and **16** in comparable yields of 51 and 54%, respectively (Scheme 3).

For the synthesis of 9-methoxy derivative **21** (Scheme 4), ketone **18**³² was reduced with sodium borohydride to afford alcohol **19** in quantitative yield. The tosyl protecting group was cleaved using activated magnesium to give secondary amine **20**

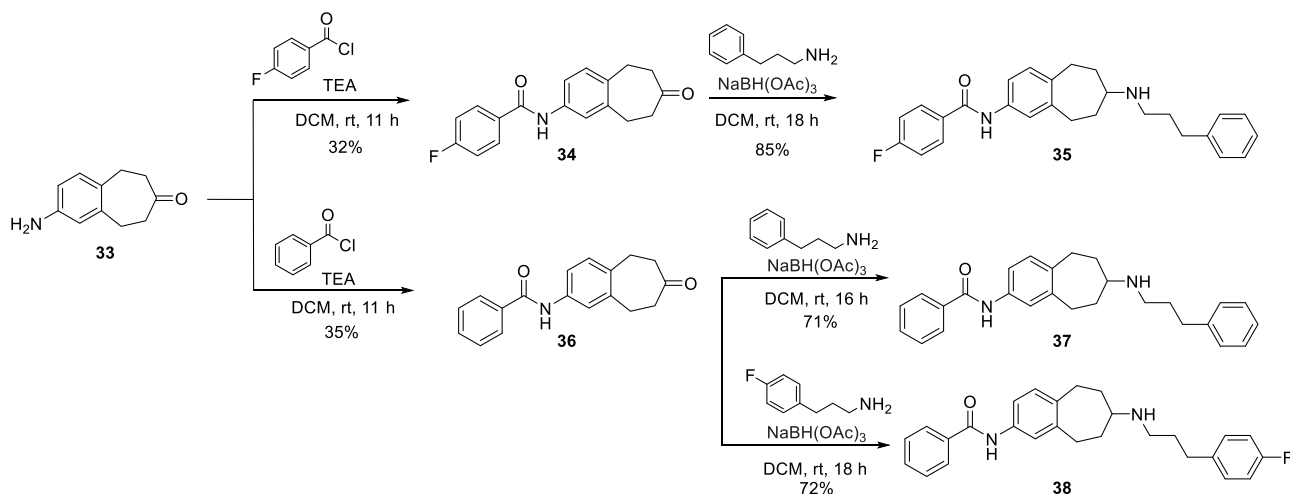
Scheme 5. Synthesis of Reference Compounds 24–28



Scheme 6. Synthesis of Reference Compounds 30–32



Scheme 7. Syntheses of Reference Compounds 35, 37, and 38

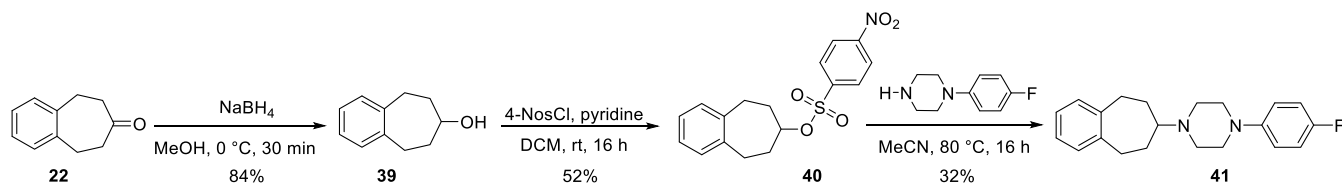


in 70% yield. In the final step, *N*-alkylation of the secondary amine **20** with [4-(4-fluorophenyl)butyl] methanesulfonate gave the reference compound **21** in 25% yield.

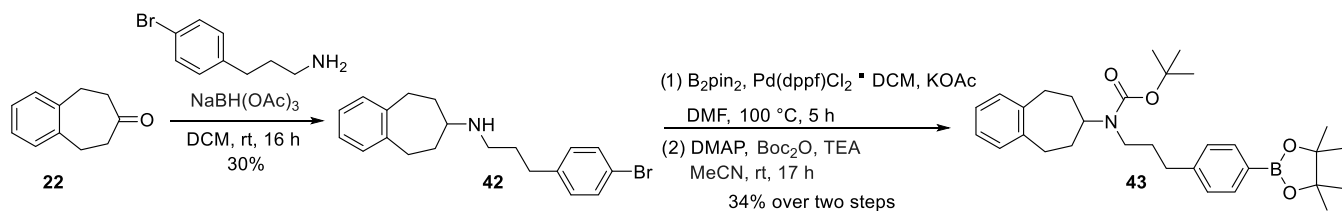
6,7,8,9-Tetrahydro-5H-benzo[7]annulen-7-amines. 6,7,8,9-Tetrahydro-5H-benzo[7]annulen-7-amines are structural analogues of 2,3,4,5-tetrahydro-1H-3-benzazepines. The key difference between the two leads is the endo or exo position of the N-atom. It was shown for 6,7,8,9-tetrahydro-

5H-benzo[7]annulen-7-amines that removal of the benzylic alcohol enhanced affinity toward the GluN2B subunit, while discarding the phenolic ether slightly increased selectivity toward GluN2B subunits.³⁸ The modification sites that we pursued are depicted in Figure 3. Conformational restriction of the linker into a piperazine ring was shown to enhance selectivity while retaining affinity.⁴⁵

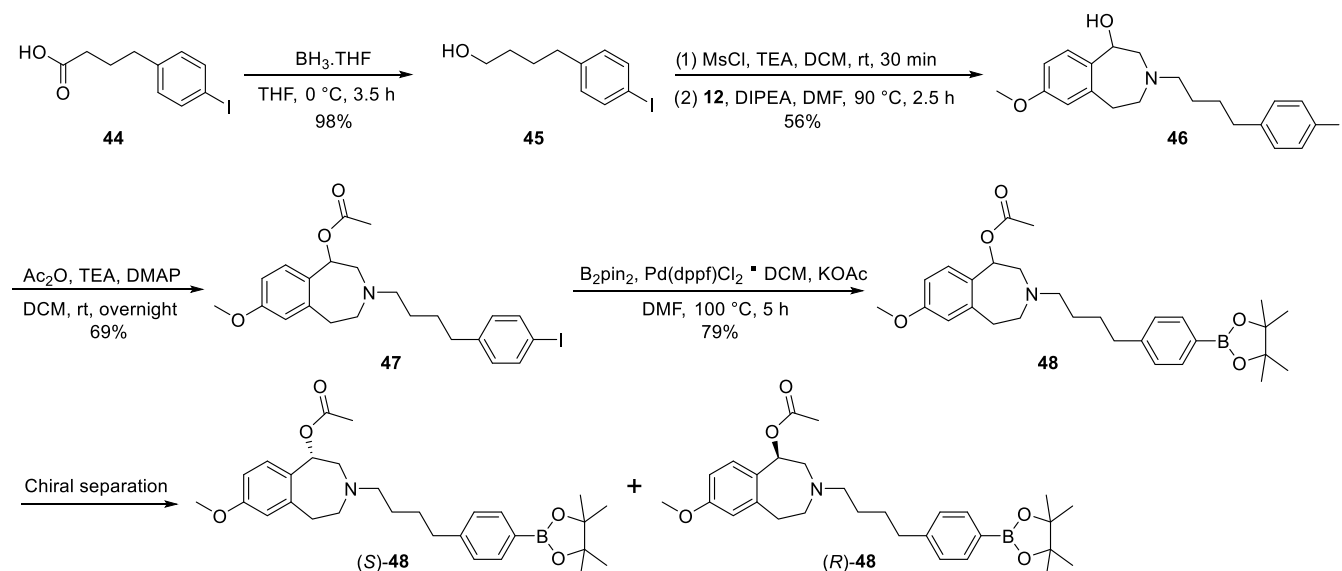
Scheme 8. Synthesis of Reference Compound 41



Scheme 9. Synthesis of Pinacol Boronic Ester 43



Scheme 10. Synthesis of Pinacol Boronic Esters 48, (S)-48, and (R)-48



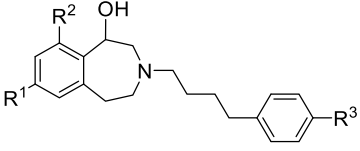
The reductive amination of the commercially available ketone **22** followed a reported procedure³⁸ that led to 6,7,8,9-tetrahydro-5H-benzo[7]annulen-7-amine derivatives **23**, **26**, and **27** in very good to excellent yields of 94, 89, and 81%, respectively (Scheme 5). Methylation of secondary amines **23** and **27** afforded the respective tertiary methylamine reference compounds **24** and **28**. To avoid overmethylation and formation of quaternary ammonium salts, Eschweiler–Clarke methylation was performed using formaldehyde and formic acid.⁴⁶ Fluoroalkylation of compound **23** using (2-fluoroethyl) tosylate gave reference compound **25** in 50% yield.

The 2-nitro compound **29**⁴⁷ (Scheme 6) was treated under reductive amination reaction conditions to generate piperazine **30** in a moderate yield of 41%. Secondary amine **31**⁴⁷ was methylated under Eschweiler–Clarke methylation conditions to afford the tertiary amine **32** in 91% yield.

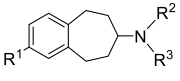
The reaction pathways leading to target compounds **35**, **37**, and **38** are depicted in Scheme 7. Acylation of primary amine **33**⁴⁸ under Schotten–Baumann conditions with the respective acid chlorides provided amides **34** and **36** in 32 and 35% yields, respectively. Further reductive amination with the corresponding primary amines led to reference compounds **35**, **37**, and **38** in 85, 71, and 72% yields, respectively.

For reference compound **41** (Scheme 8), the previous reductive amination approach of ketone **22** was not pursued because of the extremely poor yields. The previously reported explanation proposed that the unfavorable steric hindrance caused by the four methylene moieties adjacent to the intermediate iminium ion would hinder the reductive amination. However, this explanation seems to be unfounded given that the reductive amination of nitro **29** with a piperazine derivative was accomplished as depicted above in Scheme 6. A possible explanation could be that the resonance structure of the nitro group helps stabilize the flow of electrons involved in the formation of the iminium intermediate. Instead, a roundabout nucleophilic substitution strategy was followed.⁴⁵ The nucleophilic substitution of nosylate **40**⁴⁵ with the piperazine derivative afforded compound **41** in 32% yield.

Precursors for Radiosynthesis. The synthesis of the 6,7,8,9-tetrahydro-5H-benzo[7]annulen-7-amine precursor **43** for fluorine-18 labeling is depicted in Scheme 9. Reductive amination of ketone **22** afforded secondary amine **42** in 30% yield. Miyaura borylation conditions were applied to aryl bromide **42**, followed by Boc protection of the secondary amine to afford boronic ester precursor **43** in 34% yield.⁴⁹

Table 1. Binding Affinities and $\log P$ Values of 2,3,4,5-Tetrahydro-1H-3-benzazepin-1-ol Derivatives


compound	R ¹	R ²	R ³	K _i (hGluN1/GluN2B) ± SEM (nM)	K _i (σ1) ± SEM (nM)	$\log P$
Me-NB1	OCH ₃	H	H	5.4 ± 0.4	182	4.42
3	OCH ₂ CH ₂ CH ₂ F	H	H	524	174	4.90
14	OH	H	F	20 ± 4	1200	3.98
				10.4 ± 3.9 ^a	544 ^a	
(R)-14	OH	H	F	3.0 ± 1.4 ^a	1130 ^a	3.98
(S)-14	OH	H	F	42.0 ± 23.3 ^a	218 ± 8 ^a	3.98
15	OCH ₃	H	CH ₂ CH ₂ F	929	79 ± 8	4.72
16	OCH ₃	H	CH ₂ CH ₂ CH ₂ F	308	75 ± 2	5.25
21	H	OCH ₃	F	104 ± 4	420	4.56

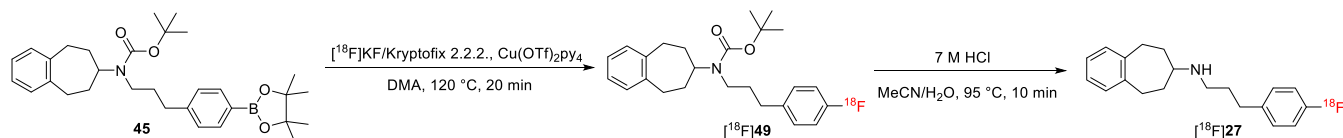
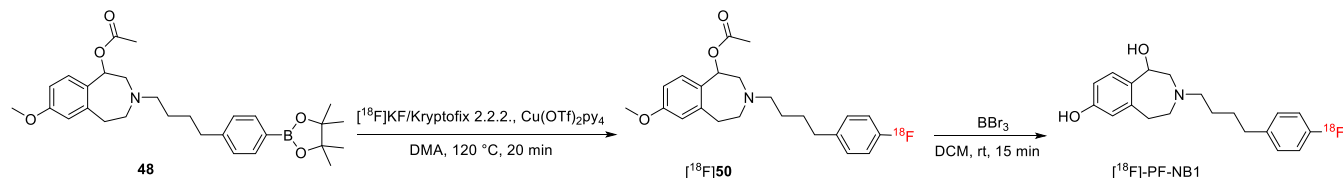
^aK_i values determined using rat brain homogenates.Table 2. Binding Affinities and $\log P$ Values for 6,7,8,9-Tetrahydro-5H-benzo[7]annulene Derivatives


compound	R ¹	R ²	R ³	K _i (hGluN1/GluN2B) ± SEM (nM)	K _i (σ1) ± SEM (nM)	K _i (σ2) ± SEM (nM)	$\log P$
24	H	CH ₃		2.3	29	162	5.44
25	H	CH ₂ CH ₂ F		4.4	119	575	5.70
26	H	H		74	475	69	4.21
27	H	H		2.1	107	255	5.05
28	H	CH ₃		6.4	17	143	5.59
32	NO ₂	CH ₃		3.0	11	76	5.19
35		H		56 ± 36	154	263	5.76
37		H		57 ± 40	390	351	5.42
38		H		179 ± 54	3000	492	5.56
30				1.8 ± 0.4	11	1.2	5.08
41				5.2	40	21	5.21

The synthetic pathway leading to pinacol boronic ester **48** precursor for radiofluorination is shown in Scheme 10. Alcohol **45**⁵⁰ was mesylated and subsequently coupled with secondary amine **12** via *N*-alkylation to afford tertiary amine **46** in 56% yield. The secondary alcohol of compound **46** was then protected with acetic anhydride to provide acetic acid ester **47** in 69% yield. Palladium-catalyzed cross-coupling of iodo **47** and bis(pinacolato)diboron in the presence of KOAc (Miyaura borylation conditions) gave pinacol boronic ester **48** in 79% yield.⁴⁹ The enantiomers of the racemic precursor **48** were separated by chiral HPLC to yield the enantiomerically pure

precursors, (*S*)- and (*R*)-**48**, as previously described for other tracers.³⁶

Structure–Affinity Relationships. 2,3,4,5-Tetrahydro-1H-3-benzazepines. The IC₅₀ values were determined experimentally and were transformed into their respective K_i values (inhibition constants reflecting the binding affinity) using the Cheng–Prusoff equation. Table 1 summarizes the K_i values for binding at GluN2B subunits and σ1Rs as well as the $\log P$ values for the 2,3,4,5-tetrahydro-1H-3-benzazepine derivatives. $\log P$ is a lipophilicity indicator and is one of the descriptors used to predict blood–brain barrier penetration.⁵¹ 2,3,4,5-Tetrahydro-1H-3-benzazepine derivatives

Scheme 11. Radiosynthesis of [^{18}F]27Scheme 12. Radiosynthesis of [^{18}F]PF-NB1

have been shown to generally exhibit high selectivity over several CNS receptors including $\sigma 2\text{Rs}$, while off-target binding to $\sigma 1\text{Rs}$ has been reported, in which case a slight structural modification can alter the binding profile of a ligand from a GluN2B subunit-binder to a $\sigma 1\text{R}$ selective ligand.³²

Elongation of the fluoroalkoxy chain at the 7-position (compound 3) diminished the affinity by 3-fold compared with the reported K_i value of 162 ± 22 nM for the fluoroethoxy analogue.⁵² The decrease in affinity follows a trend and shows that the longer the chain, the less tolerable the binding pocket seems to be.

Compound 14 (PF-NB1), which was obtained by addition of a fluorine to the phenyl ring at the para-position and cleavage of the methyl group in the 7-methoxy functionality, revealed a K_i value that approaches the reported K_i value of 14 ± 1.5 nM for NB1⁴¹ and is more than 2-fold higher than the previously reported methylated analogue compound 13 (Scheme 3).³⁶ On the other hand, selectivity over $\sigma 1\text{Rs}$ remarkably increased from the reported $\sigma 1\text{R}$ K_i value of 194 nM for NB1⁴¹ to 1200 nM for compound 14. This result was surprising considering that the methylated derivative, PF-Me-NB1, exhibited a high K_i of 12 nM toward $\sigma 1\text{Rs}$, as previously reported.³⁶ Keeping the 7-methyl ether functionality and introducing a fluoroethyl substituent at the para-position of the phenyl ring (compound 15) led to a dramatic reduction in GluN2B subunit binding affinity and loss of selectivity over $\sigma 1\text{Rs}$. Surprisingly, the fluoropropyl derivative 16 showed a 3-fold improved K_i of 308 nM relative to 15 and comparable selectivity, suggesting that the decrease in affinity could be nonsterically related. The 9-alkoxy derivative 21 showed the second-best affinity and selectivity out of this class of compounds. Since PF-NB1 outperformed all of the other 2,3,4,5-tetrahydro-1H-3-benzazepine derivatives, we separated the enantiomers and determined the K_i values of the corresponding enantiomers (S)-14 and (R)-14 as well as the racemic mixture using rat brain homogenates. The selectivity of 14 in rats was similar to that of the human GluN2B subunit with 54- and 60-fold selectivity factors, respectively. Although (R)-14 was better, all three forms still possessed suitable affinity and selectivity. Further evaluation of the 3 compounds was carried out using in vitro autoradiography after 14, (S)-14, and (R)-14 were radiolabeled with fluorine-18.

6,7,8,9-Tetrahydro-5H-benzo[7]annulen-7-amines. Table 2 summarizes the respective K_i values and $\log P$ data of the 6,7,8,9-tetrahydro-5H-benzo[7]annulen-7-amine derivatives. This class of compounds was shown to exhibit off-target binding to both $\sigma 1$ and $\sigma 2\text{Rs}$; thus, we measured the IC_{50}

values toward both receptors. The nonfluorinated analogue of compound 27 was reported to exhibit a K_i value of 16 ± 4 nM to the GluN2B subunit as well as $\sigma 1$ and $\sigma 2\text{R}$ K_i values of 150 and 27 ± 12 nM, respectively.⁴⁵ Adding a fluorine atom at the para-position of the phenyl ring in 27 had a dramatic impact on the GluN2B subunit affinity and selectivity over $\sigma 2\text{Rs}$; GluN2B subunit affinity was enhanced nearly 8-fold, while selectivity over $\sigma 2\text{R}$ soared from almost 2-fold to 120-fold. For compounds 24 and 28, selectivity over $\sigma 1\text{R}$ was lost upon methylation of the secondary amine compared with compounds 27 and 23.⁴⁵ Alkylating the secondary amine with a fluoroethyl chain in compound 25 restored the selectivity while maintaining a high binding affinity toward the GluN2B subunit, indicating that larger substituents on the secondary amine enhanced the affinity. However, we did not attempt to label this compound as it was highly lipophilic. An analogue of 24 with R^1 as OBn was recently reported to have a K_i of 3.6 ± 2.2 nM toward GluN2B as well as K_i values of 206 and 110 ± 32 nM toward $\sigma 1$ and $\sigma 2\text{Rs}$, respectively.⁴⁸ Even though this analogue possessed attractive affinity and selectivity attributes, its $\log P$ was exceedingly high (6.60); therefore, as an alternative, we substituted the OBn with a benzamide functionality. Unfortunately, the GluN2B subunit affinity was lost for compound 37. Addition of fluorine on either of the phenyl rings (compounds 35 and 38) could restore neither the affinity nor the selectivity. It is known from previous reports that the conformational restriction of the alkyl chain linker by cyclization especially using the cyclic diamine, piperazine, has a positive impact on the GluN2B subunit affinity.⁴⁵ With this in mind, we synthesized alkyl diamine derivative 26 to investigate the role of a secondary amine functionality with no conformational restriction; however, affinity toward the GluN2B subunit diminished, and selectivity over $\sigma 2\text{Rs}$ was lost. We next added a fluorine atom to the phenyl moiety of the piperazine derivative that led to compound 41; however, the fluorine effect we observed previously with regard to selectivity was greatly reduced. Furthermore, we synthesized fluorinated nitro derivatives 30 and 32 since 2-nitro derivatives were reported to exhibit high GluN2B subunit affinity.⁴⁷ Although they were highly affine, they displayed poor selectivity. From this series of compounds, we selected the best performing compound 27, which showed high GluN2B subunit binding affinity and good selectivity over $\sigma 1$ and $\sigma 2\text{Rs}$, for radiofluorination.

Radiochemistry. Radiofluorination of the boronic ester precursors followed a Cu(II)-mediated aromatic nucleophilic

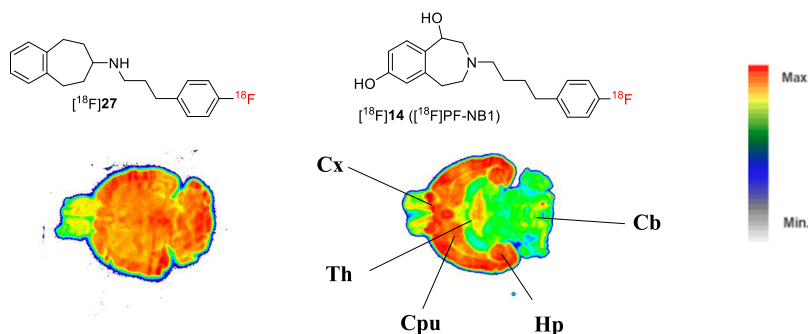


Figure 4. Representative in vitro autoradiograms of $[^{18}\text{F}]$ PF-NB and $[^{18}\text{F}]$ 27 obtained from rat coronal brain sections. Cx, cortex; Th, thalamus; Cb, cerebellum; Cpu, caudate putamen (striatum); Hp, hippocampus.

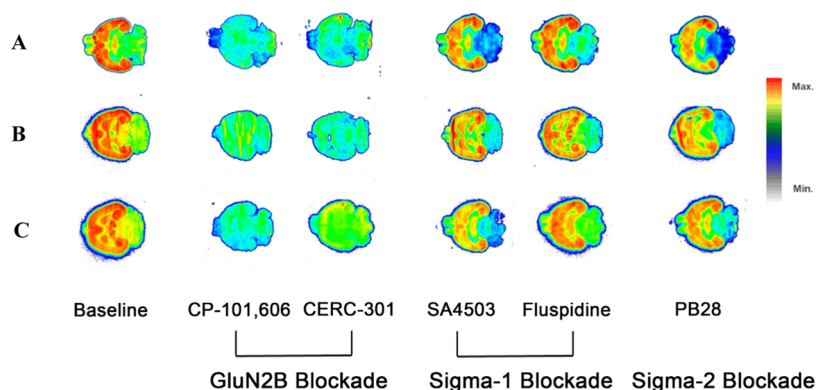


Figure 5. In vitro autoradiograms of (A) $[^{18}\text{F}]$ PF-NB1, (B) (R)- $[^{18}\text{F}]$ PF-NB1, and (C) (S)- $[^{18}\text{F}]$ PF-NB1 in rat coronal brain sections. Positive and negative control blockers were used. Solutions of 1 μM antagonists, CP-101,606 and CERC-301, were employed to establish the specificity of the tracers toward the GluN2B subunit. Solutions of 1 μM SA4503, fluspidine, and PB28 were used as negative controls to confirm selectivity to the ifenprodil binding site.

substitution reaction in analogy to a previously published procedure.⁵³

The radiosynthesis of the 6,7,8,9-tetrahydro-5H-benzo[7]-annulene tracer $[^{18}\text{F}]$ 27 depicted in Scheme 11 involved a one-pot, two-step reaction sequence encompassing radiofluorination of 45, followed by Boc removal and semipreparative HPLC purification. The radiochemical yield (RCY) of $[^{18}\text{F}]$ 27 was 54% (decay-corrected), and the molar activity amounted to 88 GBq/ μmol ($n = 1$). Radiochemical purity was greater than 95%, which was appropriate for further biological experiments. The total radiosynthesis time from the end of bombardment (EOB) until the end of synthesis was 135 min.

The radiosynthesis of $[^{18}\text{F}]$ PF-NB1 was accomplished in two steps (Scheme 12). The first step yielded intermediate $[^{18}\text{F}]$ 50 in 14–17% RCYs (decay-corrected). $[^{18}\text{F}]$ 50 was trapped on a Sep-Pak C18 Plus cartridge and eluted with absolute ethanol. The solvent was evaporated by azeotropic drying using extra-dry MeCN. This step was necessary as water quenches the Lewis acid used in the succeeding reaction. Simultaneous cleavage of the methyl and acetyl protecting groups was achieved by using BBr_3 , and the final product was purified by semipreparative HPLC. The radiosyntheses of (R)- $[^{18}\text{F}]$ PF-NB1 and (S)- $[^{18}\text{F}]$ PF-NB1 were accomplished in a similar fashion using the corresponding pinacolboronate precursors, (R)-48 and (S)-48. Radiochemical purity was greater than 95%, and molar activity amounted to 210 ± 39 GBq/ μmol ($n = 5$) for $[^{18}\text{F}]$ PF-NB1. The final product activities ranged from 0.56 to 1.2 GBq and had $4 \pm 1.1\%$ isolated RCYs (decay-corrected, $n = 5$). The total radiosyn-

thesis time from EOB until the end of synthesis was 139 min on average. The identities of $[^{18}\text{F}]$ 27, $[^{18}\text{F}]$ PF-NB1, (R)- $[^{18}\text{F}]$ PF-NB1, and (S)- $[^{18}\text{F}]$ PF-NB1 were confirmed by coinjection with their corresponding nonradioactive reference compounds.

In Vitro Autoradiography. Coronal Wistar rat whole brain sections were used to establish the in vitro binding characteristics of $[^{18}\text{F}]$ PF-NB1, (R)- $[^{18}\text{F}]$ PF-NB1, (S)- $[^{18}\text{F}]$ PF-NB1, and $[^{18}\text{F}]$ 27. While (R)- $[^{18}\text{F}]$ PF-NB1, (S)- $[^{18}\text{F}]$ PF-NB1, and $[^{18}\text{F}]$ PF-NB1 were found to accumulate heterogeneously in GluN2B-rich regions such as the cortex, thalamus, hippocampus, and striatum,⁵ $[^{18}\text{F}]$ 27 was found to bind homogeneously across the whole rat brain (Figure 4). This homogenous binding pattern can be explained by the high lipophilicity of $[^{18}\text{F}]$ 27 ($\text{clog } P = 5.05$). The high nonspecific binding exhibited by $[^{18}\text{F}]$ 27 precluded its further evaluation.

In Figure 5 are depicted the autoradiograms of (R)- $[^{18}\text{F}]$ PF-NB1, (S)- $[^{18}\text{F}]$ PF-NB1, and $[^{18}\text{F}]$ PF-NB1. The distribution of the radiotracers followed the GluN2B subunit expression profile in rats with the highest accumulation in the cortex, striatum, thalamus, and hippocampus as described in the literature.^{3,5} The lowest accumulation was detected in the cerebellum, a region with low GluN2B expression.³ Blocking experiments with GluN2B antagonists, CP-101,606 and CERC-301, confirmed the specificity of the tracers toward GluN2B. $\sigma 1\text{R}$ blockers, SA4503 and fluspidine, as well as $\sigma 2\text{R}$ blocker PB28, did not compete with either $[^{18}\text{F}]$ PF-NB1, (R)- $[^{18}\text{F}]$ PF-NB1, or (S)- $[^{18}\text{F}]$ PF-NB1 binding, suggesting that none of the three radiotracers binds to $\sigma 1\text{R}$ or $\sigma 2\text{R}$. Contrary

to previous results from our group, we did not observe a notable difference between the two enantiomers with regard to selectivity and specificity. We selected racemic [^{18}F]PF-NB1 for further in vivo testing given the remarkable autoradiograms, which obviates the need for tedious chiral separation.

In Vivo PET Imaging. *PET Imaging in Wistar Rats.* Dynamic PET imaging was performed on anesthetized Wistar rats for 90 min under baseline conditions, and for blocking experiments, CP-101,606 (1, 3, 5, and 10 mg/kg, GluN2B $\text{IC}_{50} = 11 \text{ nM}$ ⁵⁴) was injected 1 min before the intravenous injection of [^{18}F]PF-NB1. Figure 6 shows coronal, sagittal, and

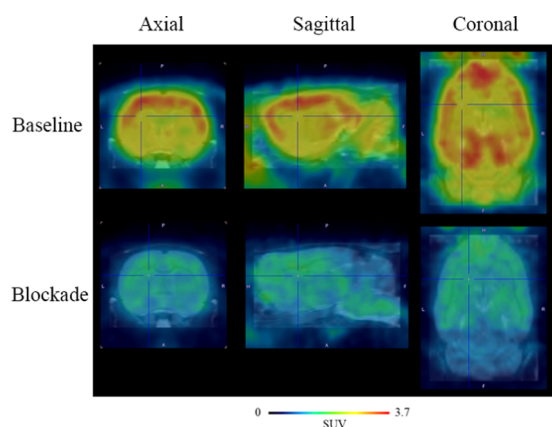


Figure 6. In vivo PET images of [^{18}F]PF-NB1 in rat brain under baseline and blockade (10 mg/kg CP-101,606 injected 1 min before radiotracer injection) conditions superimposed on the MRI template (PMOD). PET images were averaged from 30 to 90 min post tracer injection. The color bar indicates standardized uptake value (SUV, calculated as accumulated radioactivity (Bq) per g tissue divided by injected dose per body weight).

axial images of the rat brain under baseline and blockade conditions. Under baseline conditions, a heterogeneous accumulation of [^{18}F]PF-NB1 in the rat brain, which is consistent with the known expression pattern of GluN2B subunits in the brain, was observed. This accumulation was inhibited by the GluN2B antagonist, CP-101,606, suggesting specific binding of [^{18}F]PF-NB1 to GluN2B subunit-containing NMDARs.

The corresponding time–activity curves (TACs) comparing tracer uptake under baseline and blockade conditions are shown in Figure 7A. TACs for specific brain regions were generally higher in the cortex, hippocampus, striatum, and thalamus relative to the cerebellum (Supporting Information, Figure 2). There was a remarkable difference in the washout rate between [^{18}F]PF-NB1 and the previously reported [^{11}C]Me-NB1, (R)-[^{11}C]Me-NB1, and (R)-[^{18}F]OF-Me-NB1,^{31,33,36} in which case the washout rate of [^{18}F]PF-NB1 was slower than the other radiotracers so far reported in our group. Using CP-101,606, an experimental GluN2B targeting drug that showed efficacy in clinical trials,^{12,55,56} we assessed concentration-dependent receptor occupancy of CP-101,606 at doses spanning between 1 and 10 mg/kg (Figure 7B).

A dose-dependent decrease of the SUVs with increasing CP-101,606 doses was observed (Figure 7A). The SUVs were then used to determine the in vivo receptor occupancy of CP-101,606 (Figure 7B). The CP-101,606 dose required for 50% receptor occupancy (D_{50}) was found to be $31 \mu\text{mol/kg}$. This study shows the utility of [^{18}F]PF-NB1 in (1) visualizing target engagement of GluN2B targeting drugs in vivo and (2) estimating the required doses for GluN2B targeting drugs.

PET Imaging in Wild-Type and $\sigma 1\text{R}$ Knockout Mice. To assess whether [^{18}F]PF-NB1 exhibits off-target binding to $\sigma 1\text{Rs}$ in vivo, pilot dynamic PET scans were performed using $\sigma 1\text{R}$ knockout ($\sigma 1\text{R-KO}$) and wild-type (WT) CD1 mice for 90 min. The resulting TACs are depicted in Figure 8. The

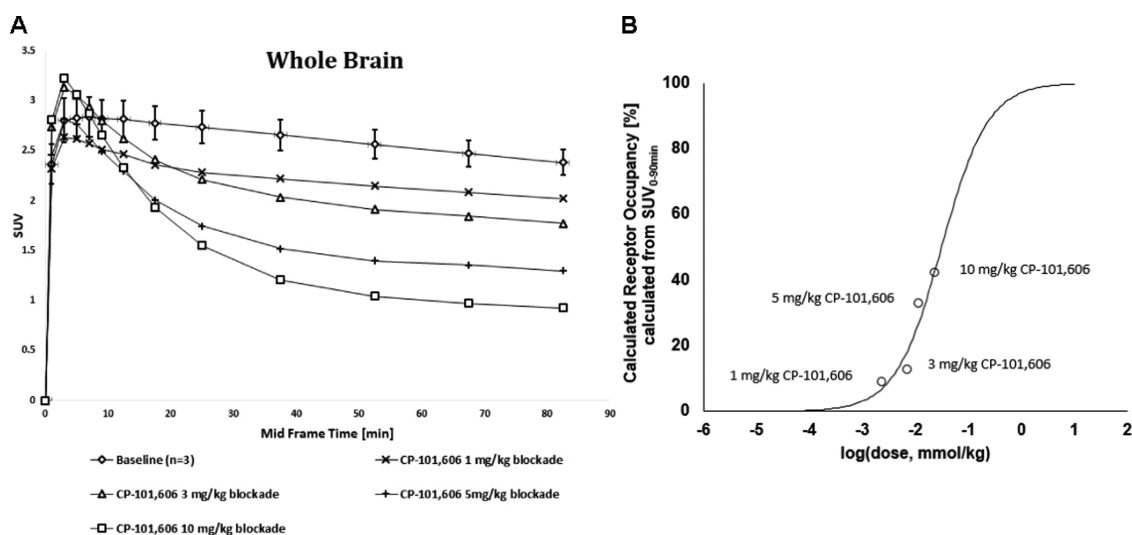


Figure 7. (A) TACs representing whole brain accumulation of [^{18}F]PF-NB1 ($n = 3$) presented as standardized uptake values (SUVs) from tracer injection to 90 min postinjection. The specificity of binding and dose dependency was confirmed by the injection of different doses of the GluN2B antagonist, CP-101,606 (1, 3, 5, and 10 mg/kg) ($n = 1$). (B) Receptor occupancy of the clinically experimental GluN2B antagonist CP-101,606 using [^{18}F]PF-NB1 in Wistar rats calculated from experimental PET imaging of 90 min SUVs. A D_{50} of $31 \mu\text{mol/kg}$ was determined. The following equations were used to calculate the receptor occupancy: (1) $\text{AUC} = (b_{\text{max}} - b_{\text{min}}) \times D_{50} / (D + D_{50}) + b_{\text{min}}$. (2) $\text{RO} = (b_{\text{max}} - \text{AUC}) / (b_{\text{max}} - b_{\text{min}}) \times 100$, where AUC is defined as the area under the curve of the respective PET scan, D_{50} is the dose required to be injected to achieve 50% receptor occupancy, D is the actual dose, RO is the receptor occupancy in %, and b_{max} and b_{min} are the maximum and minimum binding, respectively.

TACs of [^{18}F]PF-NB1 were found to be similar in both $\sigma 1\text{R}$ -KO and WT mice, indicating that the brain uptake of [^{18}F]PF-NB1 is $\sigma 1\text{R}$ -independent.

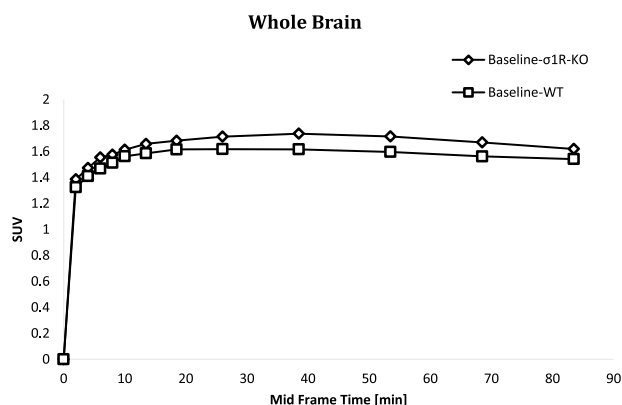


Figure 8. Typical TACs representing the whole brain uptake of [^{18}F]PF-NB1 in $\sigma 1\text{R}$ -KO and WT mice.

We conclude from these experiments that [^{18}F]PF-NB1 exhibits high in vivo selectivity of binding to GluN2B subunits over $\sigma 1\text{R}$. Furthermore, these results confirm the in vitro selectivity observed from binding affinity determinations and the in vitro autoradiography experiments using fluspidine, and SA4503 as $\sigma 1\text{R}$ blocking agents.

Metabolite Studies. Previous tracers assessed by our group from the 2,3,4,5-tetrahydro-1*H*-3-benzazepine class of compounds showed no brain radiometabolites.^{33,36} To verify that this holds true for the new radioligand, [^{18}F]PF-NB1 was injected into male Wistar rats, and blood samples at 5, 15, 30, 45, and 60 min postinjection, as well as brain extracts at 15, 30, and 60 min, were taken and analyzed by radio-ultra-performance liquid chromatography (UPLC). The analysis showed only the presence of the intact parent radiotracer in the brain up to 60 min postinjection. In Supporting Information, Figure 3 are depicted the chromatograms of the brain extracts. In blood, 3 radiometabolites, which were more polar than the parent radioligand, were detected. At later time points, the detection of radiometabolites was not possible due to low radioactivity levels in the blood. This may be explained by fast clearance of the radiotracer from the blood.

Biodistribution Studies. Ex vivo baseline ($n = 4$) and blockade ($n = 4$) biodistribution experiments were carried out at 45 min postinjection of [^{18}F]PF-NB1 in male Wistar rats using eliprodil as a GluN2B blocker. The 45 min postinjection time point was selected based on the TACs of the baseline PET scans. Similar to the PET results, [^{18}F]PF-NB1 displayed heterogeneous uptake in brain regions known to contain high densities of GluN2B subunits with the cortex and thalamus exhibiting the highest uptake. Compared with these brain regions, the cerebellum showed a lower uptake of [^{18}F]PF-NB1: cortex/cerebellum (1.2, $p = 0.0003$), striatum/cerebellum (1.1, $p = 0.0045$), and thalamus/cerebellum (1.1, $p = 0.014298$). Both brain and body ex vivo biodistribution results are summarized in the Supporting Information, Tables 1 and 2.

CONCLUSIONS

We have successfully designed and synthesized a series of 2,3,4,5-tetrahydro-1*H*-3-benzazepines and 6,7,8,9-tetrahydro-

5*H*-benzo[7]annulen-7-amines as GluN2B subunit ligands and investigated their binding affinities toward GluN2B subunits as well as their selectivity over σRs . For the most promising compounds, a robust radiosynthesis was established to afford [^{18}F]PF-NB1, (*R*)-[^{18}F]PF-NB1, (*S*)-[^{18}F]PF-NB1, and [^{18}F] 27 in good radiochemical yields, high molar activities, and excellent radiochemical purities. Although 6,7,8,9-tetrahydro-5*H*-benzo[7]annulen-7-amines showed high affinity and selectivity, they lacked the necessary structural polar features that would label them as potential GluN2B imaging agents, and thus this class of compounds would require further optimization strategies. [^{18}F]PF-NB1 is the first radiolabeled racemic 2,3,4,5-tetrahydro-1*H*-3-benzazepine-1,7-diol derivative that shows high GluN2B subunit selectivity and specificity. The use of [^{18}F]PF-NB1 will obviate the need to perform labor-intensive chiral HPLC separation. [^{18}F]PF-NB1 exhibited good in vivo performance in PET imaging studies performed in rats and showed a remarkably slower washout compared with our first-generation 2,3,4,5-tetrahydro-1*H*-3-benzazepine-1-ol tracers with no confounding brain radiometabolites. The results of the receptor occupancy with the experimental GluN2B therapeutic drug CP-101,606 revealed a dose dependency of blockade by [^{18}F]PF-NB1. Taken together, the results show that [^{18}F]PF-NB1 is a promising fluorine-18 PET tracer with potential for clinical translation for the imaging of the GluN2B subunits of the NMDARs and has utility for studying GluN2B subunit receptor occupancy.

EXPERIMENTAL SECTION

Reagents and solvents were purchased from Sigma-Aldrich Chemie GmbH (Germany), Acros Organics (Belgium), Fluka (Switzerland), Merck (Germany), Chemieliva (China), Manchester Organics (U.K.), or ABCR GmbH (Germany) and were used without further purification steps. The purchased solvents were of anhydrous grade (puriss, dried over molecular sieves, $\text{H}_2\text{O} < 0.005\%$) unless stated otherwise. Solvents necessary for extractions, column chromatography, and thin-layer chromatography (TLC) were acquired as technical grade. Nonaqueous reactions were generally performed under a nitrogen atmosphere using flame-dried glassware and standard syringe/septa methods. Reactions were magnetically stirred and further monitored by TLC performed on Merck TLC glass sheets (silica gel 60 F254). TLC Spots were visualized with UV light ($\lambda = 254\text{ nm}$). Chromatographic purification of products was performed using SiliaFlash P60 silica gel (Silicycle) for preparative column chromatography (particle size 40–63 μm). Reactions at 0°C were carried out using an ice/water bath for cooling purposes.

The $\log P$ values were calculated using CambridgeSoft software, ChemDraw 15.0 (Perkin-Elmer). ^1H and ^{13}C NMR spectra were recorded on a Bruker Avance FT-NMR spectrometer (400 MHz), and the chemical shifts (δ) are presented in ppm referenced to tetramethylsilane (0 ppm). All coupling constants (J) are reported in this work in Hz. Multiplicities in the ^1H NMR spectra are generally given as either s, singlet; d, doublet; dd, doublet of doublet; t, triplet; dt, doublet of triplet; m, multiplet; or br, broad peak. All ^{13}C NMR spectra measured were completely proton decoupled.

High-resolution mass spectrometry (HRMS) was conducted on a Bruker maXis (ESI-Qq-TOF-MS) spectrometer (Bruker Daltonik GmbH, Germany), and the resulting data is reported in m/z . Preparative HPLC of the final compounds 3, 14, 15, 16, and 21 was conducted with a Merck-Hitachi L7150 pump system and an Ultimate XB-C18 column (150 mm \times 21.2 mm, 5 mm) using a gradient system of 10 mM aq. NH_4HCO_3 (solvent A) and MeCN (solvent B); 0.0–5.0 min, 20% B; 5.1–15.0 min, 20–50% B; 15.1–20.0 min, 50% B; 20.1–28.0 min, 50–95% B; 28.1–35.0 min, 95% B; 35.1–37.0 min, 95–20% B; 37.1–45.0 min, 20% B, with a flow rate of 10 mL/min and UV detection signal at 230 nm. For compounds 24, 25, 26, 27,

28, 30, 32, 35, 37, 38, and 41, the purity was determined using analytical HPLC on a Merck Hitachi system comprising a D-7000 interface, an L-7100 pump, an L-7400 UV detector, and Ultimate XB-C18 (4.6 mm × 150 mm, 3 μm) using generally a gradient system of 0.1% aq. trifluoroacetyl (TFA) (solvent A) and MeCN (solvent B); 0.0–7.0 min, 30–50% B; 7.1–15.0 min, 50% B; 15.1–20.0 min, 50–60% B; 20.1–21.0 min, 60–95% B; 21.1–26.0 min, 95% B; 26.1–27.0 min, 95–30% B; 27.1–32.0 min, 30% B with a flow rate of 1 mL/min and UV detection signal at 254 nm. Enantiomeric purification of racemic precursor 48 was performed by semipreparative HPLC and a Reprosil Chiral-normal phase column (8 μm, 250 mm × 10 mm) using an isocratic system of hexane (solvent A) and isopropanol (solvent B); 0.0–60.0 min, 2% B. Purification of the radiotracers was performed on a semipreparative Merck-Hitachi L2130 HPLC system equipped with a radiation detector VRM 202 (Cameca, The Netherlands). For the purification of (R)-, (S)- and [¹⁸F]PF-NB1, an Agilent Eclipse XDB-C18 (9.4 mm × 250 mm, 5 μm) column was used with the following gradient solvent system: 0.1% aq. H₃PO₄ (solvent A), MeCN (solvent B); 0.0–5.0 min, 20% B; 5.1–25.0 min, 20–40% B; 25.1–28.0 min, 40% B; 28.1–30.0 min, 40–60% B; 30.1–33.0 min, 60–90% B; 33.1–36.0 min, 90% B; 36.1–38.0 min, 90–20% B; 38.1–42.0 min, 20% B. A flow rate of 4 mL/min was used, and the UV signal was detected at 230 nm. For quality control, an aliquot of the final formulation was injected into an analytical Agilent 1100 HPLC system mounted with a Raytest Gabi Star radiodetector and an Atlantis T3 C18 reversed-phase column (4.6 mm × 150 mm, 3 μm). The analysis gradient system was as follows: 0.1% aq. TFA (solvent A), MeCN (solvent B); 0.0–10.0 min, 40–60% B; 10.1–11.0 min, 60–40% B; 11.1–15.0 min, 40% B, flow rate 1 mL/min and UV detection at 230 nm. For the semipreparative HPLC purification of [¹⁸F]27, an ACE-C18 column (250 mm × 10 mm, 5 μm) was used with the following conditions: 0.1% aq. H₃PO₄ (solvent A), MeCN (solvent B); 0.0–4.0 min, 20% B; 4.1–20.0 min, 20–60% B; 20.1–23.0 min, 60% B; 23.1–28.0 min, 60–80% B; 28.1–29.0 min, 80–5% B; 29.1–34.0 min, 5% B; 34.1–35.0 min, 5–20% B; 35.1–38.0 min, 20% B with a flow rate of 4 mL/min and UV detection signal of 230 nm. For quality control, an aliquot from the final formulation was injected on a reversed-phase column (LiChroCART 250-4, LiChrospher RP-18, 5 μm) with a flow rate of 1 mL/min and applying the following conditions: 0.1% aq. TFA (solvent A), MeCN (solvent B); 0.0–2.0 min, 30% B; 2.1–15.0 min, 30–60% B; 15.1–17.1 min, 60% B; 17.1–20.1 min, 60–80% B; 20.1–21.1 min, 80–95% B; 21.1–25.1 min, 95% B; 25.1–26.0 min, 95–30% B; 26.1–28.1 min, 30% B with UV signal detection at 230 nm. Molar activity was calculated by comparing the UV intensity of the formulated products against calibration curves of the corresponding cold references of known concentrations. Purity of all biologically tested compounds was ≥95%. Intermediates 23,⁴⁵ 29,⁴⁷ 31,⁴⁷ 33,⁴⁸ 39,⁴⁵ 40,⁴⁵ and 45⁵⁰ were synthesized according to the published literature.

Chemistry. 3-(4-Phenylbutyl)-2,3,4,5-tetrahydro-1H-benzo[d]-azepine-1,7-diol (2, NB1). To a solution of commercially available 1 (1.00 equiv, 170 mg, 0.522 mmol) in dichloromethane (DCM) (7.2 mL), BBr₃ (7.30 equiv, 3.80 mL, 1 M in DCM, 3.80 mmol) was added dropwise at –78 °C. The reaction mixture was warmed to rt and subsequently stirred for 4 h. Afterward, the reaction mixture was poured into ice water (36 mL), and the organic phase was completely evaporated under reduced pressure. The resultant mixture was diluted with distilled water (100 mL) and subsequently extracted with DCM (3 × 100 mL). The combined organic layers were dried over anhydrous magnesium sulfate and concentrated under reduced pressure. The crude was purified by preparative HPLC to give compound 2 (100 mg, 0.318 mmol, 61%). ¹H NMR (400 MHz, CDCl₃): δ 1.50–1.71 (m, 4H), 2.40 (t, J = 12.1 Hz, 1H), 2.49 (d, J = 12.06 Hz, 1H), 2.56–2.67 (m, 5H), 2.98 (dd, J₁ = 6.0 Hz, J₂ = 12.3 Hz, 1H), 3.11–3.28 (m, 2H), 4.57 (d, J = 6.7 Hz, 1H), 6.53–6.58 (m, 2H), 7.01 (d, J = 7.7, 1H), 7.15–7.21 (m, 3H), 7.27–7.31 (m, 2H). ¹³C NMR (100 MHz, CDCl₃): δ 26.7, 29.2, 36.7, 56.2, 59.7, 60.8, 72.5, 112.5, 117.6, 125.9, 128.5, 128.6, 130.1, 135.4, 141.5, 142.4,

155.2. HRMS (ESI) calculated for C₂₀H₂₆NO₂ [M + H]⁺ 312.1958, found 312.1958.

7-(3-Fluoropropoxy)-3-(4-phenylbutyl)-2,3,4,5-tetrahydro-1H-benzo[d]azepine-1-ol (3). To a stirred solution of 2 (1.00 equiv, 33.0 mg, 0.106 mmol) in dimethylformamide (DMF, 0.4 mL), 3-fluoropropyl tosylate (1.22 equiv, 30.0 mg, 0.129 mmol) and K₂CO₃ (1.5 equiv, 24.0 mg, 0.159 mmol) were added. The reaction mixture was stirred at 120 °C for 6 h and subsequently diluted with a mixture of water and MeCN (1:1, 4.6 mL). The crude residue was purified by preparative HPLC, and the title compound 3 was obtained as a white solid (30.0 mg, 0.081 mmol, 76% yield). ¹H NMR (400 MHz, CDCl₃): δ 7.33–7.23 (m, 2H), 7.21–7.15 (m, 3H), 7.11 (d, J = 7.8 Hz, 1H), 6.68–6.62 (m, 2H), 4.67 (t, J = 6.9 Hz, 1H), 4.60–4.53 (m, 2H), 4.29–4.11 (s, br, 1H), 4.07 (t, J = 6.9 Hz, 2H), 3.30–3.21 (m, 1H), 3.19–3.11 (m, 1H), 3.02–2.95 (m, 1H), 2.69–2.56 (m, 5H), 2.50 (d, J = 12.1 Hz, 1H), 2.40 (t, J = 11.9 Hz, 1H), 2.22–2.07 (m, 2H), 1.70–1.50 (m, 4H). ¹³C NMR (100 MHz, CDCl₃): δ 158.2, 149.1, 148.4, 142.4, 141.3, 129.7, 128.4, 128.0, 125.9, 120.4, 117.2, 111.0, 80.8 (d, J = 164.5), 72.4, 63.5, 60.9, 56.1, 36.9, 35.9, 31.0, 30.5, 29.2, 26.7. HRMS (ESI) calculated for C₂₃H₃₁FO₂ [M + H]⁺ 372.2333, found 372.2337.

4-(4-Methoxy-4-oxobutanoyl)phenethyl methyl succinate (5a). To an ice-cooled mixture of commercially available 4a (1.00 equiv, 6.90 mL, 57.3 mmol) in DCM (64 mL) was added portionwise aluminum trichloride (1.20 equiv, 9.17 g, 68.8 mmol), followed by methyl 4-chloro-4-oxobutylate (1.10 equiv, 7.80 mL, 63.0 mmol). The mixture was stirred at 0 °C for 30 min, quenched with ice water (400 mL), and extracted with DCM (3 × 300 mL). The combined organic layers were washed with brine (2 × 150 mL) and dried over anhydrous magnesium sulfate. Solvents were removed under reduced pressure to give the methyl phenethyl succinate quantitatively. Methyl phenethyl succinate (1.00 equiv, 12.8 g, 54.3 mmol) was stirred at 0 °C in DCM (60 mL) before adding aluminum trichloride (5.50 equiv, 39.8 g, 299 mmol) portionwise, followed by methyl 4-chloro-4-oxobutylate (1.30 equiv, 8.70 mL, 70.6 mmol). The mixture was stirred at 0 °C for 30 min, quenched with ice water (300 mL) and extracted with DCM (3 × 200 mL). The combined organic layers were washed with brine (2 × 100 mL) and dried over anhydrous magnesium sulfate, and solvents were removed under reduced pressure. The resulting crude was purified by flash column chromatography (silica gel; Hex/EtOAc 6:4) to give 5a (14.0 g, 40.2 mmol, 74%). ¹H NMR (400 MHz, CDCl₃): δ 2.59 (s, 4H), 2.75 (t, J = 6.5 Hz, 2H), 2.99 (t, J = 6.5 Hz, 2H), 3.29 (t, J = 6.5 Hz, 2H), 3.66 (s, 3H), 3.69 (s, 3H), 4.32 (t, J = 7.0 Hz, 2H), 7.31 (d, J = 8.2 Hz, 2H), 7.92 (d, J = 8.2 Hz, 2H). ¹³C NMR (100 MHz, CDCl₃): δ 28.1, 28.9, 29.1, 33.4, 35.1, 51.9, 52.0, 64.6, 128.4, 129.2, 135.1, 143.7, 172.3, 172.8, 173.3, 197.7. HRMS (ESI) calculated for C₁₈H₂₃O₇ [M + H]⁺ 351.1438, found 351.1442.

3-(4-(4-Methoxy-4-oxobutanoyl)phenyl)propyl Methyl Succinate (5b). To an ice-cooled mixture of commercially available 4b (1.00 equiv, 3.00 mL, 22.0 mmol) in DCM (25 mL) was added portionwise aluminum trichloride (1.20 equiv, 3.52 g, 26.4 mmol), followed by the addition of methyl 4-chloro-4-oxobutylate (1.10 equiv, 3.00 mL, 24.2 mmol). The mixture was stirred at 0 °C for 30 min, quenched with ice water (300 mL), and extracted with DCM (3 × 200 mL). The combined organic layers were washed with brine (2 × 100 mL) and dried over anhydrous magnesium sulfate. Solvents were removed under reduced pressure to yield methyl (3-phenylpropyl) succinate quantitatively. Methyl (3-phenylpropyl) succinate (1.00 equiv, 5.64 g, 22.5 mmol) was then dissolved in DCM (25 mL) at 0 °C before the portionwise addition of aluminum trichloride (3.20 equiv, 9.61 g, 72.1 mmol) and methyl 4-chloro-4-oxobutylate (1.30 equiv, 3.60 mL, 29.3 mmol) was carried out. The mixture was stirred at 0 °C for 30 min, quenched with ice water (400 mL), and extracted with DCM (3 × 200 mL). The combined organic layers were washed with brine (2 × 100 mL) and dried over anhydrous magnesium sulfate. Solvents were removed under reduced pressure, and the residue was purified by flash column chromatography (silica gel; Hex/EtOAc 6:4) to give 5b (4.29 g, 11.7 mmol, 52%). ¹H NMR (400 MHz, CDCl₃): δ 1.92–2.02 (m, 2H), 2.63 (s, 4H), 2.71–2.78 (m, 4H), 3.3 (t, J = 6.8 Hz, 2H), 3.68

(s, 3H), 3.69 (s, 3H), 4.11 (t, $J = 6.5$ Hz, 2H), 7.27 (d, $J = 8.3$ Hz, 2H), 7.91 (d, $J = 8.3$ Hz, 2H). ^{13}C NMR (100 MHz, CDCl_3): $\delta = 28.2, 29.0, 29.2, 29.9, 32.3, 33.4, 51.9, 52.0, 64.0, 128.5, 128.8, 134.8, 147.2, 172.3, 172.9, 173.5, 197.7$. HRMS (ESI) calculated for $\text{C}_{19}\text{H}_{25}\text{O}_7$ [$\text{M} + \text{H}$] $^+$ 365.1595, found 365.1595.

4-(4-(2-Hydroxyethyl)phenyl)-4-oxobutanoic Acid (6a). To a stirred solution of aq. NaOH (30%, 35 mL) and MeOH (526 mL) was added **5a** (1.00 equiv, 14.0 g, 40.0 mmol). The reaction mixture was heated to reflux and stirred for 20 min. The pH was adjusted to 7 using conc. HCl (37% w/w in water), and the volatiles were evaporated under reduced pressure. The resulting mixture was diluted with aq. HCl (0.03 M, 300 mL) and extracted with EtOAc (3×300 mL). The combined organic layers were dried over anhydrous magnesium sulfate, and the solvents were evaporated under reduced pressure to give the title compound **6a** (11.9 g, 40.0 mmol, quant.). ^1H NMR (400 MHz, $(\text{CD}_3)_2\text{CO}$): δ 2.71 (t, $J = 6.4$ Hz, 2H), 2.88 (t, $J = 6.70$ Hz, 2H), 3.30 (t, $J = 6.3$ Hz, 2H), 3.80 (t, $J = 6.8$ Hz, 2H), 7.39 (d, $J = 8.3$ Hz, 2H), 7.94 (d, $J = 8.3$ Hz, 2H). ^{13}C NMR (100 MHz, $(\text{CD}_3)_2\text{CO}$): δ 28.2, 33.7, 40.0, 63.2, 128.6, 130.0, 135.8, 146.3, 173.7, 198.2. HRMS (ESI) calculated for $\text{C}_{12}\text{H}_{14}\text{NaO}_4$ [$\text{M} + \text{Na}$] $^+$ 245.0784, found 245.0783.

4-(4-(3-Hydroxypropyl)phenyl)-4-oxobutanoic Acid (6b). To a stirred solution of aq. NaOH (30%, 7.2 mL) and MeOH (108 mL) was added **5b** (3.00 g, 8.23 mmol). The reaction mixture was heated to reflux and stirred for 20 min. The pH was adjusted to 7 using conc. HCl, and the volatiles were evaporated under reduced pressure. The resulting mixture was diluted with aq. HCl (0.03 M, 300 mL) and extracted with EtOAc (3×300 mL). The combined organic layers were dried over anhydrous magnesium sulfate, and the solvents were evaporated under reduced pressure to give the title compound **6b** (2.57 g, 8.23 mmol, quant.). ^1H NMR (400 MHz, $(\text{CD}_3)_2\text{CO}$): δ 1.79–1.88 (m, 2H), 2.70 (t, $J = 6.5$ Hz, 2H), 2.77 (t, $J = 7.5$ Hz, 2H), 3.29 (t, $J = 6.5$ Hz, 2H), 3.57 (t, $J = 6.3$ Hz, 2H), 7.37 (d, $J = 8.3$ Hz, 2H), 7.94 (d, $J = 8.3$ Hz, 2H). ^{13}C NMR (100 MHz, $(\text{CD}_3)_2\text{CO}$): δ 28.0, 32.5, 33.6, 34.7, 61.2, 128.6, 129.3, 135.4, 148.9, 174.0, 198.0. HRMS (ESI) calculated for $\text{C}_{13}\text{H}_{16}\text{NaO}_4$ [$\text{M} + \text{Na}$] $^+$ 259.0941, found 259.0944.

4-(4-(2-Hydroxyethyl)phenyl)butanoic Acid (7a). To a solution of **6a** (1.00 equiv, 9.29 g, 41.8 mmol) in water (50 mL), zinc (7.00 equiv, 19.1 g, 293 mmol) was added portionwise. Conc. HCl (21 mL) was added dropwise, and the reaction mixture was refluxed for 1 h. The mixture was diluted with aq. HCl (0.03 M, 350 mL) and extracted with EtOAc (3×350 mL). The combined organic layers were dried over anhydrous magnesium sulfate, and solvents were removed under reduced pressure. The residue was purified by flash column chromatography (silica gel; Hex/EtOAc 6:4, 1% AcOH) to give a mixture of the inseparable olefin and **7a**. Therefore, the mixture (4.18 g) and Pd/C (10%, 1.01 g, 10.7 mmol) were suspended in MeOH (53 mL) and stirred at rt for 1 h under a H_2 atmosphere. The mixture was then filtered through a pad of celite and washed with MeOH (5×20 mL). The filtrate was concentrated in vacuo to afford compound **7a** (4.04 g, 19.4 mmol, 49%). ^1H NMR (400 MHz, $(\text{CD}_3)_2\text{CO}$): δ 1.84–1.93 (m, 2H), 2.30 (t, $J = 7.4$ Hz, 2H), 2.62 (t, $J = 7.4$ Hz, 2H), 2.77 (t, $J = 7.1$ Hz, 2H), 3.73 (t, $J = 7.1$ Hz, 2H), 7.12 (d, $J = 8.1$ Hz, 2H), 7.16 (d, $J = 8.1$ Hz, 2H). ^{13}C NMR (100 MHz, $(\text{CD}_3)_2\text{CO}$): δ 27.6, 33.6, 35.3, 39.9, 64.0, 129.2, 129.9, 138.0, 140.3, 173.8. HRMS (ESI) calculated for $\text{C}_{12}\text{H}_{16}\text{NaO}_3$ [$\text{M} + \text{Na}$] $^+$ 231.0992, found 231.0991.

4-(4-(3-Hydroxypropyl)phenyl)butanoic Acid (7b). To a solution of **6b** (1.00 equiv, 1.76 g, 7.46 mmol) in water (8.6 mL), zinc (7 equiv, 3.410 g, 52.2 mmol) was added portionwise. Conc. HCl (3.7 mL) was added dropwise, and the reaction mixture was refluxed for 1 h. The mixture was diluted with aq. HCl (0.03 M, 250 mL) and extracted with EtOAc (3×250 mL). The combined organic layers were dried over anhydrous magnesium sulfate, and solvents were removed under reduced pressure. The residue was purified by flash column chromatography (silica gel; Hex/EtOAc 6:4, 1% AcOH) to give an inseparable mixture of **7b** and the olefin. The mixture (1.52 g) and Pd/C (10%, 0.345 g, 3.24 mmol) were suspended in MeOH (18 mL) and stirred at rt for 1 h under a H_2 atmosphere. The mixture was

then filtered through a pad of celite and washed with MeOH (5×20 mL). The filtrate was concentrated in vacuo to afford compound **7b** (1.57 g, 7.07 mmol, 79%). ^1H NMR (400 MHz, $(\text{CD}_3)_2\text{CO}$): δ 1.74–1.92 (m, 4H), 2.27 (t, $J = 7.4$ Hz, 2H), 2.58–2.66 (m, 4H), 3.54 (t, $J = 6.2$ Hz, 2H), 7.11 (br s, 4H). ^{13}C NMR (100 MHz, $(\text{CD}_3)_2\text{CO}$): δ 27.0, 31.7, 33.1, 34.6, 34.8, 61.1, 128.5, 128.5, 139.3, 140.1, 174.5. HRMS (ESI) calculated for $\text{C}_{13}\text{H}_{18}\text{NaO}_3$ [$\text{M} + \text{Na}$] $^+$ 245.1148, found 245.1148.

Methyl 4-(4-(2-((Methylsulfonyl)oxy)ethyl)phenyl)butanoate (8a). To a solution of **7a** (1.00 equiv, 2.20 g, 10.6 mmol) in DCM (211 mL) was added dropwise methanesulfonyl chloride (5.00 equiv, 4.10 mL, 52.8 mmol), followed by the addition of tetraethylammonium (TEA, 2.00 equiv, 2.90 mL, 21.1 mmol). The mixture was stirred at rt for 30 min, diluted with EtOAc (150 mL), washed with aq. HCl (0.03 M, 3×300 mL), and dried over anhydrous magnesium sulfate. Solvents were removed under reduced pressure and the residue was purified by flash column chromatography (silica gel; Hex/EtOAc 7:3, 1% AcOH) to obtain the title compound **8a** (672 mg, 2.32 mmol, 22%). ^1H NMR (400 MHz, $(\text{CD}_3)_2\text{CO}$): δ 1.84–1.93 (m, 2H), 2.31 (t, $J = 7.5$ Hz, 2H), 2.63 (t, $J = 7.9$ Hz, 2H), 2.98 (s, 3H), 3.03 (t, $J = 6.7$ Hz, 2H), 3.61 (s, 3H), 4.42 (t, $J = 6.8$ Hz, 2H), 7.17 (d, $J = 8.1$ Hz, 2H), 7.24 (d, $J = 8.1$ Hz, 2H). ^{13}C NMR (100 MHz, $(\text{CD}_3)_2\text{CO}$): δ 27.4, 33.6, 35.2, 35.7, 37.0, 51.5, 71.5, 129.4, 129.9, 135.4, 141.1, 173.9. HRMS (ESI) calculated for $\text{C}_{14}\text{H}_{21}\text{O}_5\text{S}$ [$\text{M} + \text{H}$] $^+$ 301.1104, found 301.1105.

Methyl 4-(4-(3-((Methylsulfonyl)oxy)propyl)phenyl)butanoate (8b). To a solution of **7b** (1.00 equiv, 1.57 g, 7.07 mmol) in DCM (141 mL) was added dropwise methanesulfonyl chloride (5.00 equiv, 2.70 mL, 35.3 mmol), followed by the addition of TEA (2.00 equiv, 2.00 mL, 14.1 mmol). The mixture was stirred at rt for 30 min, diluted with EtOAc (150 mL), washed with aq. HCl (0.03 M, 3×150 mL), and dried over anhydrous magnesium sulfate. Solvents were removed under reduced pressure and the residue was purified by flash column chromatography (silica gel; Hex/EtOAc 7:3, 1% AcOH) to obtain the title compound **8b** (974 mg, 3.11 mmol, 44%). ^1H NMR (400 MHz, $(\text{CD}_3)_2\text{CO}$): δ 1.83–1.93 (m, 2H), 1.99–2.07 (m, 2H), 2.30 (t, $J = 7.4$ Hz, 2H), 2.61 (t, $J = 8.0$ Hz, 2H), 2.71 (t, $J = 8.0$ Hz, 2H), 3.07 (s, 3H), 3.60 (s, 3H), 4.23 (t, $J = 6.4$ Hz, 2H), 7.13 (d, $J = 8.3$ Hz, 2H), 7.17 (d, $J = 8.0$ Hz, 2H). ^{13}C NMR (100 MHz, $(\text{CD}_3)_2\text{CO}$): δ 27.6, 31.7, 31.9, 33.8, 35.3, 37.2, 51.6, 70.5, 129.4, 129.5, 139.4, 140.4, 174.0. HRMS (ESI) calculated for $\text{C}_{15}\text{H}_{22}\text{NaO}_5\text{S}$ [$\text{M} + \text{Na}$] $^+$ 337.1080, found 337.1080.

Methyl 4-(4-(2-Fluoroethyl)phenyl)butanoate (9a). To a solution of **8a** (1.00 equiv, 1.00 g, 3.33 mmol) in *tert*-amyl alcohol (12 mL), CsF (3.00 equiv, 1.52 g, 9.99 mmol) was added portionwise. The mixture was stirred at 80 °C for 6 h, cooled to rt, diluted with water (200 mL), and extracted with DCM (3×200 mL). The combined organic layers were dried over anhydrous magnesium sulfate, followed by the removal of solvents under reduced pressure. The residue was purified by flash column chromatography (silica gel; Hex/EtOAc 95:5) to give the title product **9a** (190 mg, 0.83 mmol, 25%). ^1H NMR (400 MHz, $(\text{CD}_3)_2\text{CO}$): δ 1.84–1.93 (m, 2H), 2.31 (t, $J = 7.4$ Hz, 2H), 2.62 (t, $J = 7.9$ Hz, 2H), 2.94 (t, $J = 6.5$ Hz, 1H), 2.99 (t, $J = 6.5$ Hz, 1H), 3.61 (s, 3H), 4.55 (t, $J = 6.5$ Hz, 1H), 4.67 (t, $J = 6.5$ Hz, 1H), 7.15 (d, $J = 8.3$ Hz, 2H), 7.20 (d, $J = 8.0$ Hz, 2H). ^{13}C NMR (100 MHz, $(\text{CD}_3)_2\text{CO}$): δ 27.6, 33.8, 35.3, 37.2, 51.6, 84.9, 129.5, 129.9, 136.1, 140.9, 174.0. HRMS (EI) calculated for $\text{C}_{13}\text{H}_{17}\text{FO}_2$ [M^+] 224.1207, found 224.1210.

Methyl 4-(4-(3-Fluoropropyl)phenyl)butanoate (9b). A mixture of kryptofix 2.2.2 (3.30 equiv, 3.75 g, 9.95 mmol), KF (3.30 equiv, 578 mg, 9.95 mmol), and **8b** (1.00 equiv, 948 mg, 3.02 mmol) was dissolved in MeCN (38 mL) and stirred at 90 °C for 1 h. Afterward, the mixture was poured into water (200 mL) and extracted with DCM (3×200 mL). The combined organic layers were dried over anhydrous magnesium sulfate and concentrated in vacuo. The crude product was purified by flash column chromatography (silica gel; Hex/EtOAc 95:5) to afford **9b** (238 mg, 3.28 mmol, 33%). ^1H NMR (400 MHz, $(\text{CD}_3)_2\text{CO}$): δ 1.84–1.92 (m, 2H), 1.93–2.03 (m, 2H), 2.31 (t, $J = 7.5$ Hz, 2H), 2.61 (t, $J = 7.8$ Hz, 2H), 2.69 (t, $J = 8.0$ Hz, 2H), 3.61 (s, 3H), 4.38 (t, $J = 6.0$ Hz, 1H), 4.50 (t, $J = 6.0$ Hz, 1H),

7.14 (br s, 4H). ^{13}C NMR (100 MHz, $(\text{CD}_3)_2\text{CO}$): δ 27.7, 31.6, 33.0, 33.8, 35.4, 51.6, 84.0, 129.4, 129.5, 139.9, 140.3, 174.1. HRMS (EI) calculated for $\text{C}_{14}\text{H}_{19}\text{FO}_2$ [M^{+}] 238.1364, found 238.1366.

4-(4-(2-Fluoroethyl)phenyl)butan-1-ol (10a). To a solution of **9a** (1.00 equiv, 182 mg, 0.812 mmol) in tetrahydrofuran (THF, 1.4 mL) was added lithium aluminum hydride (2.00 equiv, 62.0 mg, 1.62 mmol) at 0 °C. The mixture was then allowed to stir at rt for 30 min. The resulting mixture was diluted with water (100 mL) and extracted with DCM (3×100 mL). The combined organic layers were dried over anhydrous magnesium sulfate and the solvents were evaporated under reduced pressure to give **10a** (165 mg, 0.812 mmol, quant.). ^1H NMR (400 MHz, $(\text{CD}_3)_2\text{CO}$): δ 1.49–1.57 (m, 2H), 1.62–1.71 (m, 2H), 2.60 (t, $J = 7.7$ Hz, 2H), 2.93 (t, $J = 6.5$ Hz, 1H), 2.98 (t, $J = 6.5$ Hz, 1H), 3.41 (t, $J = 5.3$ Hz, 1H), 3.52–3.58 (m, 2H), 4.54 (t, $J = 6.1$ Hz, 1H), 4.66 (t, $J = 6.1$ Hz, 1H), 7.14 (d, $J = 8.1$ Hz, 2H), 7.18 (d, $J = 8.1$ Hz, 2H). ^{13}C NMR (100 MHz, $(\text{CD}_3)_2\text{CO}$): δ 28.8, 33.4, 36.0, 37.2, 62.4, 84.9, 129.4, 129.8, 135.6, 141.8. HRMS (EI) calculated for $\text{C}_{12}\text{H}_{17}\text{FO}$ [M^{+}] 196.1258, found 196.1256.

4-(4-(3-Fluoropropyl)phenyl)butan-1-ol (10b). To a solution of **9b** (1.00 equiv, 232 mg, 0.974 mmol) in THF (1.5 mL), lithium aluminum hydride (2.00 equiv, 73.9 mg, 1.95 mmol) was added portionwise at 0 °C. The mixture was then allowed to stir at rt for 30 min. The resulting mixture was diluted with water (250 mL) and extracted with DCM (3×250 mL). The combined organic layers were dried over anhydrous magnesium sulfate and the solvents were evaporated under reduced pressure to give **10b** (160 mg, 0.760 mmol, 78%). ^1H NMR (400 MHz, $(\text{CD}_3)_2\text{CO}$): δ 1.49–1.58 (m, 2H), 1.58–1.62 (m, 2H), 1.89–2.03 (m, 2H), 2.59 (t, $J = 7.9$ Hz, 2H), 2.68 (t, $J = 7.9$ Hz, 2H), 3.41 (t, $J = 5.4$ Hz, 1H), 3.52–3.58 (m, 2H), 4.38 (t, $J = 6.0$ Hz, 1H), 4.50 (t, $J = 6.0$ Hz, 1H), 7.13 (s, 4H). ^{13}C NMR (100 MHz, $(\text{CD}_3)_2\text{CO}$): δ 28.8, 31.6, 33.1, 33.5, 36.0, 62.4, 83.9, 129.2, 129.4, 139.5, 141.2. HRMS (EI) calculated for $\text{C}_{13}\text{H}_{19}\text{FO}$ [M^{+}] 210.1414, found 210.1412.

4-(4-(2-Fluoroethyl)phenyl)butyl Methanesulfonate (11a). To a solution of **10a** (1.00 equiv, 160 mg, 0.815 mmol) in DCM (16 mL), methanesulfonyl chloride (5.00 equiv, 0.32 mL, 4.08 mmol) was added dropwise. After 5 min of stirring at rt, TEA (2.00 equiv, 0.23 mL, 1.63 mmol) was added, and the reaction mixture was allowed to stir for an additional 30 min at rt. The mixture was diluted with EtOAc (100 mL), washed with aq. HCl (0.03 M, 3×100 mL), and dried over anhydrous magnesium sulfate. Solvents were removed under reduced pressure and the crude was purified by flash column chromatography (silica gel; Hex/EtOAc 8:2) to obtain the title compound **11a** (184 mg, 0.668 mmol, 82%). ^1H NMR (400 MHz, $(\text{CD}_3)_2\text{CO}$): δ 1.69–1.79 (m, 4H), 2.65 (t, $J = 7.2$ Hz, 2H), 2.93 (t, $J = 6.4$ Hz, 1H), 2.99 (t, $J = 6.4$ Hz, 1H), 3.06 (s, 3H), 4.26 (t, $J = 6.2$ Hz, 2H), 4.54 (t, $J = 6.5$ Hz, 1H), 4.67 (t, $J = 6.5$ Hz, 1H), 7.17 (d, $J = 8.3$ Hz, 2H), 7.20 (d, $J = 8.3$ Hz, 2H). ^{13}C NMR (100 MHz, $(\text{CD}_3)_2\text{CO}$): δ 28.2, 29.5, 35.5, 37.1, 37.3, 71.1, 84.9, 129.4, 129.9, 136.0, 141.2. HRMS (ESI) calculated for $\text{C}_{13}\text{H}_{23}\text{FNO}_3\text{S}$ [$\text{M} + \text{NH}_4$] $^{+}$ 292.1377, found 292.1380.

4-(4-(3-Fluoropropyl)phenyl)butyl Methanesulfonate (11b). To a solution of **10b** (1.00 equiv, 157 mg, 0.747 mmol) in DCM (15 mL), methanesulfonyl chloride (5 equiv, 0.29 mL, 3.73 mmol) was added dropwise. After 5 min of stirring at rt, TEA (2.00 equiv, 0.21 mL, 1.49 mmol) was added, and the reaction mixture was allowed to stir for an additional 30 min at rt. The mixture was diluted with EtOAc (100 mL), washed with aq. HCl (0.03 M, 3×100 mL), and dried over anhydrous magnesium sulfate. The solvents were removed under reduced pressure and the crude was purified by flash column chromatography (silica gel; Hex/EtOAc 8:2) to obtain the title compound **11b** (193 mg, 0.672 mmol, 90%). ^1H NMR (400 MHz, $(\text{CD}_3)_2\text{CO}$): δ 1.69–1.81 (m, 4H), 1.81–1.90 (m, 2H), 2.62–2.71 (m, 4H), 3.06 (s, 3H), 4.25 (t, $J = 6.0$ Hz, 2H), 4.38 (t, $J = 5.9$ Hz, 1H), 4.50 (t, $J = 5.9$ Hz, 1H), 7.15 (s, 4H). ^{13}C NMR (100 MHz, $(\text{CD}_3)_2\text{CO}$): δ 28.3, 29.5, 31.6, 33.0, 35.5, 37.1, 71.1, 83.8, 129.3, 129.4, 139.7, 140.6. HRMS: calculated for $\text{C}_{14}\text{H}_{25}\text{FNO}_3\text{S}$ [$\text{M} + \text{NH}_4$] $^{+}$ 306.1534, found 306.1534.

3-(4-(4-Fluorophenyl)butyl)-7-methoxy-2,3,4,5-tetrahydro-1H-benzo[d]azepin-1-ol (13). To a solution of commercially available

amine **12** (1.00 equiv, 30.0 mg, 0.155 mmol) in DMF (0.5 mL) was added *N,N*-diisopropylethylamine (0.90 equiv, 24.0 μL , 0.140 mmol). The resulting mixture was stirred for 5 min at rt, and 4-(4-fluorophenyl)butyl methanesulfonate (0.90 equiv, 34.0 mg, 0.140 mmol) in DMF (0.5 mL) was subsequently added dropwise. The resulting solution was stirred at 90 °C for 3 h and diluted with a mixture of water and MeCN (1:1, 4.5 mL). Purification was performed by preparative HPLC to give the title compound **13** as a white solid (26.0 mg, 0.076 mmol, 49%). ^1H NMR (400 MHz, CDCl_3): δ 7.16–7.07 (m, 3H), 7.00–6.93 (m, 2H), 6.68–6.62 (m, 2H), 4.57 (d, $J = 6.9$ Hz, 1H), 3.78 (s, 3H), 3.31–3.26 (m, 1H), 3.19–3.11 (m, 1H), 3.02–2.95 (m, 1H), 2.69–2.56 (m, 5H), 2.50 (d, $J = 12.1$ Hz, 1H), 2.40 (t, $J = 11.9$ Hz, 1H), 1.70–1.49 (m, 4H), signal for the OH is not visible. ^{13}C NMR (100 MHz, CDCl_3): δ 161.4 (d, $J = 243.1$ Hz), 159.1, 141.4, 138.0, 135.7, 129.8 (d, $J = 9.2$ Hz, 3C), 116.8, 115.17 (d, $J = 21.5$ Hz, 2C), 110.4, 72.6, 61.0, 59.7, 56.3, 55.3, 37.1, 35.1, 29.4, 26.8. HRMS (ESI) calculated for $\text{C}_{21}\text{H}_{27}\text{FNO}_2$ [$\text{M} + \text{H}$] $^{+}$ 344.2020, found 344.2023.

3-(4-(4-Fluorophenyl)butyl)-2,3,4,5-tetrahydro-1H-benzo[d]azepine-1,7-diol (14, PF-NB1). Compound **13** (1.00 equiv, 118 mg, 0.343 mmol) was dissolved in DCM (5.0 mL), followed by dropwise addition of BBr_3 in DCM (7.30 equiv, 1 M, 2.5 mL, 2.50 mmol) while cooling the reaction mixture to –78 °C. The resulting mixture was stirred for 4 h at rt and subsequently quenched by the addition of ice water (5.0 mL). DCM was evaporated under reduced pressure, and an extraction was performed with aq. NaOH (1 M, 25 mL) and ethyl acetate (3×25 mL). The combined organic layers were concentrated under reduced pressure, and the resulting crude was purified by preparative HPLC to give the title compound **14** (30.0 mg, 0.085 mmol, 61% yield). ^1H NMR (400 MHz, CDCl_3): δ 7.15–7.07 (m, 2H), 7.00–6.92 (m, 3H), 6.53–6.46 (m, 2H), 5.70–5.15 (s, br, 2H), 4.57 (d, $J = 6.9$ Hz, 1H), 3.22–3.08 (m, 2H), 2.99–2.88 (m, 1H), 2.69–2.50 (m, 6H), 2.40 (t, $J = 11.9$ Hz, 1H), 1.70–1.49 (m, 4H). ^{13}C NMR (100 MHz, CDCl_3): δ 161.4 (d, $J = 243.1$), 155.8, 141.3, 138.0, 134.6, 130.0, 129.8 (d, $J = 8.4$ Hz, 2C), 117.8, 115.2 (d, $J = 21.6$ Hz, 2C), 112.7, 72.6, 61.0, 59.7, 56.3, 36.5, 35.1, 29.4, 26.7. HRMS (ESI) calculated for $\text{C}_{20}\text{H}_{23}\text{FNO}_2$ [$\text{M} + \text{H}$] $^{+}$ 330.1864, found 330.1864.

3-(4-(4-(2-Fluoroethyl)phenyl)butyl)-7-methoxy-2,3,4,5-tetrahydro-1H-benzo[d]azepin-1-ol (15). To a solution of commercially available amine **12** (1.00 equiv, 30.0 mg, 0.155 mmol) in DMF (0.5 mL) was added dropwise *N,N*-diisopropylethylamine (0.90 equiv, 24 μL , 0.140 mmol), and the resulting mixture was stirred for 5 min at rt. A solution of 4-(4-(2-fluoroethyl)phenyl)butyl methanesulfonate (0.90 equiv, 38.0 mg, 0.140 mmol) in DMF (0.5 mL) was added dropwise. The resulting mixture was stirred at 90 °C for 3 h and subsequently diluted with water and MeCN (1:1, 4.5 mL). Purification was carried out by preparative HPLC to give the title compound **15** (29.0 mg, 0.078 mmol, 51% yield). ^1H NMR (400 MHz, CDCl_3): δ 7.18–7.05 (m, 5H), 6.67–6.62 (m, 2H), 4.68 (t, $J = 6.7$ Hz, 1H), 4.60–4.53 (m, 2H), 3.78 (s, 3H), 3.31–3.21 (m, 1H), 3.19–3.11 (m, 1H), 3.06–2.95 (m, 3H), 2.70–2.56 (m, 5H), 2.50 (d, $J = 12.1$ Hz, 1H), 2.40 (t, $J = 11.9$ Hz, 1H), 1.70–1.50 (m, 4H), signal for the OH is not visible. ^{13}C NMR (100 MHz, CDCl_3): δ 159.1, 141.4, 140.8, 135.7, 134.5, 129.8, 129.1 (2C), 128.7 (2C), 116.8, 110.4, 84.3 (d, $J = 168.8$), 72.6, 61.0, 59.7, 56.3, 55.3, 37.1, 35.1, 31.0, 29.4, 26.8. HRMS (ESI) calculated for $\text{C}_{23}\text{H}_{31}\text{FNO}_2$ [$\text{M} + \text{H}$] $^{+}$ 372.2333, found 372.2338.

3-(4-(4-(3-Fluoropropyl)phenyl)butyl)-7-methoxy-2,3,4,5-tetrahydro-1H-benzo[d]azepin-1-ol (16). Commercially available amine **12** (1.00 equiv, 30.0 mg, 0.155 mmol) was dissolved in DMF (0.5 mL), followed by the dropwise addition of *N,N*-diisopropylethylamine (0.90 equiv, 24 μL , 0.140 mmol), and the resulting mixture was stirred for 5 min at rt. A solution of 4-(4-(3-fluoropropyl)phenyl)butyl methanesulfonate (0.90 equiv, 40.0 mg, 0.140 mmol) in DMF (0.5 mL) was added dropwise. The resulting mixture was stirred at 90 °C for 3 h and subsequently diluted with water and MeCN (1:1, 4.5 mL). Purification was carried out by preparative HPLC to give the title compound **16** (32.0 mg, 0.083 mmol, 54% yield). ^1H NMR (400 MHz, CDCl_3): δ 7.18–7.09 (m, 5H), 6.68–6.62 (m, 2H), 4.56 (d, $J =$

6.9 Hz, 1H), 4.46 (dt, $J_1 = 47.1$ Hz, $J_2 = 5.8$ Hz, 2H), 3.78 (s, 3H), 3.31–3.21 (m, 1H), 3.19–3.11 (m, 1H), 3.06–3.00 (m, 1H), 2.72 (t, $J = 7.6$ Hz, 2H), 2.68–2.56 (m, 5H), 2.50 (d, $J = 12.1$ Hz, 1H), 2.40 (t, $J = 11.9$ Hz, 1H), 2.08–1.92 (m, 2H), 1.70–1.50 (m, 4H), signal for the OH is not visible. ^{13}C NMR (100 MHz, CDCl_3): δ 159.1, 141.4, 140.7, 138.6, 135.8, 129.8, 128.6 (2C), 128.6 (2C), 116.8, 110.4, 83.3 (d, $J = 164.6$), 72.6, 61.0, 59.7, 56.3, 55.3, 37.1, 36.6, 35.1, 32.3, 29.8, 26.8. HRMS (ESI) calculated for $\text{C}_{24}\text{H}_{33}\text{FNO}_2$ $[\text{M} + \text{H}]^+$ 386.2490, found 386.2492.

9-Methoxy-3-tosyl-2,3,4,5-tetrahydro-1H-benzo[d]azepin-1-one (18). The synthesis and purification of ketone **18** were performed according to the published procedure but with minor modifications.³² Acid **17** (1.00 equiv, 50.0 g, 138 mmol) was dissolved in DCM (500 mL), and the solution was cooled to 0 °C. Subsequent addition of P_2O_5 (5.00 equiv, 98.0 g, 690 mmol) and stirring at 0 °C for 24 h was followed by addition of NaOH (3%) to give a pH of 13 and extraction with DCM (3 \times 500 mL). Purification with flash column chromatography (silica gel; DCM:EtOAc 20:1) and iterative recrystallization from EtOH gave the title compound **18** (920 mg, 2.67 mmol, 11% yield). ^1H NMR (400 MHz, CDCl_3): δ 7.47–7.42 (m, 2H), 7.33–7.27 (m, 1H), 7.18–7.12 (m, 2H), 6.78 (d, $J = 7.8$, 1H), 6.70 (d, $J = 7.8$, 1H), 4.09 (s, 2H), 3.76 (s, 3H), 3.53 (t, $J = 6.9$, 2H), 2.82 (t, $J = 6.9$, 2H), 2.39 (s, 3H). ^{13}C NMR (100 MHz, CDCl_3): δ 202.5, 157.6, 143.2, 137.8, 135.9, 133.1, 129.8 (2C), 126.9 (2C), 126.2, 120.7, 111.1, 55.9, 55.4, 46.6, 32.1, 21.7. HRMS (ESI) calculated for $\text{C}_{18}\text{H}_{20}\text{NO}_4\text{S}$ $[\text{M} + \text{H}]^+$ 346.1108, found 346.1105.

9-Methoxy-3-tosyl-2,3,4,5-tetrahydro-1H-benzo[d]azepin-1-ol (19). Compound **18** (1.00 equiv, 450 mg, 1.30 mmol) was suspended in MeOH (6.8 mL), and NaBH_4 (2.00 equiv, 99.0 mg, 2.61 mmol) was added portionwise to the suspension. The reaction mixture was stirred for 2 h at rt. The solvent was evaporated under reduced pressure. Subsequently, water (250 mL) was added, and an extraction was carried out with DCM (3 \times 250 mL). The combined organic layers were dried over anhydrous magnesium sulfate and then concentrated under reduced pressure to give the title compound **19** (440 mg, 1.27 mmol, 97% yield). ^1H NMR (400 MHz, CDCl_3): δ 7.70–7.62 (m, 2H), 7.33–7.27 (m, 2H), 7.17–7.12 (m, 1H), 6.78 (d, $J = 7.8$, 1H), 6.67 (d, $J = 7.8$, 1H), 5.61 (d, $J = 6.9$, 1H), 4.09–4.00 (m, 1H), 3.94–3.87 (m, 1H), 3.79 (s, 3H), 3.48–3.39 (m, 1H), 3.53, 3.12–3.05 (m, 1H), 2.95–2.74 (m, 3H), 2.38 (s, 3H). ^{13}C NMR (100 MHz, CDCl_3): δ 157.6, 143.2, 140.3, 135.9, 129.8 (2C), 129.1, 128.6, 126.9 (2C), 122.9, 109.7, 64.2, 55.9, 51.0, 48.1, 35.2, 21.7. HRMS (ESI) calculated for $\text{C}_{18}\text{H}_{21}\text{NNaO}_4\text{S}$ $[\text{M} + \text{Na}]^+$ 370.1083, found 370.1083.

9-Methoxy-2,3,4,5-tetrahydro-1H-benzo[d]azepin-1-ol (20). To a stirred solution of **19** (1.00 equiv, 190 mg, 0.547 mmol) in MeOH (12 mL) was added activated Mg (50.0 equiv, 664 mg, 27.3 mmol) portionwise, and the reaction mixture was refluxed for 24 h. The reaction mixture was filtered, followed by the addition of aq. HCl (0.1 M, 2.0 mL). The solvents were evaporated under reduced pressure, and the crude was redissolved in DCM (200 mL). Aq. NaOH (3%) was added, and the aqueous phase was extracted with DCM (3 \times 200 mL). The combined organic layers were dried over magnesium sulfate and evaporated under reduced pressure. The crude product was purified by flash column chromatography (silica gel; DCM/MeOH 8:2, 4% triethylamine) to yield the title compound **20** (74.0 mg, 0.383 mmol, 70% yield). ^1H NMR (400 MHz, CDCl_3): δ 7.13–7.06 (m, 1H), 6.75 (d, $J = 7.8$, 1H), 6.67 (d, $J = 7.8$, 1H), 5.51 (d, $J = 6.9$, 1H), 3.79 (s, 3H), 3.40–3.32 (m, 2H), 3.29–3.22 (m, 1H), 2.95–2.73 (m, 3H), signals for the OH and NH are not visible. ^{13}C NMR (100 MHz, CDCl_3): δ 157.6, 143.2, 131.4, 129.1, 122.9, 109.7, 64.2, 55.9, 52.8, 49.4, 38.9. HRMS (ESI) calculated for $\text{C}_{11}\text{H}_{16}\text{NO}_2$ $[\text{M} + \text{H}]^+$ 194.1176, found 194.1177.

3-(4-(4-fluorophenyl)butyl)-9-methoxy-2,3,4,5-tetrahydro-1H-benzo[d]azepin-1-ol (21). To a stirred solution of **20** (1.00 equiv, 20.0 mg, 0.103 mmol) in DMF (0.5 mL) was added dropwise DIPEA (0.90 equiv, 16 μL , 0.093 mmol). The resulting mixture was stirred for 5 min at rt before 4-(4-fluorophenyl)butyl methanesulfonate (0.90 equiv, 23.0 mg, 0.093 mmol) in DMF (0.5 mL) was added dropwise. The resulting solution was stirred at 90 °C for 3 h and diluted with a

mixture of water and MeCN (1:1, 4.5 mL). Purification was performed by preparative HPLC to give the title compound **21** (9.0 mg, 0.026 mmol, 25% yield). ^1H NMR (400 MHz, CDCl_3): δ 7.15–7.07 (m, 3H), 6.99–6.92 (m, 2H), 6.75 (d, $J = 7.8$, 1H), 6.67 (d, $J = 7.8$, 1H), 5.51 (d, $J = 6.9$ Hz, 1H), 3.80 (s, 3H), 3.36–3.27 (m, 1H), 3.26–3.19 (m, 1H), 3.07–3.00 (m, 1H), 2.71–2.55 (m, 5H), 2.42 (d, $J = 12.1$ Hz, 1H), 2.35 (t, $J = 11.9$ Hz, 1H), 1.70–1.50 (m, 4H), signal for the OH is not visible. ^{13}C NMR (100 MHz, CDCl_3): δ 161.3 (d, $J = 243.1$), 157.6, 142.1, 138.0, 131.4, 129.8, 129.8, 128.4, 122.9, 115.3, 115.1, 109.7, 62.3, 60.1, 59.7, 56.1, 56.1, 37.1, 35.1, 29.4, 26.8. HRMS (ESI) calculated for $\text{C}_{21}\text{H}_{27}\text{FNO}_2$ $[\text{M} + \text{H}]^+$ 344.2020, found 344.2022.

N-Methyl-N-(3-phenylpropyl)-6,7,8,9-tetrahydro-5H-benzo[7]-annulen-7-amine (24). Formic acid (10.0 equiv, 118 μL , 3.08 mmol) was added to a solution of **23** (1.00 equiv, 86.0 mg, 0.308 mmol) in formaldehyde (10.0 equiv, 229 μL , 3.08 mmol), which was refluxed at 100 °C for 16 h. The solvent was subsequently evaporated under reduced pressure and diluted with 2 M aq. NaOH (100 mL), which was extracted with chloroform (4 \times 100 mL). The combined organic layers were washed with brine (200 mL), dried over anhydrous sodium sulfate, filtered, and concentrated under reduced pressure. The resulting crude was purified via flash column chromatography (silica gel; Hex/EtOAc 6:4) to yield the title compound **24** (72.0 mg, 0.245 mmol, 80% yield). ^1H NMR (400 MHz, CDCl_3): δ 7.31–7.26 (m, 2H), 7.23–7.15 (m, 3H), 7.15–7.09 (m, 4H), 2.84–2.61 (m, 7H), 2.50–2.41 (m, 2H), 2.23 (s, 3H), 2.11–2.02 (m, 2H), 1.80 (p, $J = 7.6$ Hz, 2H), 1.43–1.30 (m, 2H). ^{13}C NMR (101 MHz, CDCl_3): δ 142.8 (2C), 142.6, 129.0 (2C), 128.5 (2C), 128.4 (2C), 126.4 (2C), 125.8, 67.8, 53.3, 37.8, 33.8, 33.6 (2C), 30.3, 30.0 (2C). HRMS (ESI) calculated for $\text{C}_{21}\text{H}_{28}\text{N}$ $[\text{M} + \text{H}]^+$ 294.2216, found 294.2218.

N-(2-Fluoroethyl)-N-(3-phenylpropyl)-6,7,8,9-tetrahydro-5H-benzo[7]annulen-7-amine (25). 2-Fluoroethyl 4-methylbenzenesulfonate (1.50 equiv, 176 mg, 0.805 mmol) and Cs_2CO_3 (1.50 equiv, 262 mg, 0.805 mmol) were added to a solution of **23** (1.00 equiv, 150 mg, 0.537 mmol) in DMF (0.4 mL). The solution was left to stir overnight at 90 °C. Thereafter, the reaction mixture was diluted with ice-cold water (110 mL) and extracted with DCM (3 \times 35 mL). Afterward, the combined organic layers were washed with brine (50 mL), dried over anhydrous sodium sulfate, filtered, and concentrated at 65 °C under reduced pressure. The crude was purified via flash column chromatography (silica gel; DCM) to yield the title compound **25** (88.0 mg, 0.270 mmol, 50% yield). ^1H NMR (400 MHz, CDCl_3): δ 7.19–7.13 (m, 2H), 7.10–7.01 (m, 7H), 4.49 (d, $J = 47.6$ Hz, 2H), 4.34–3.92 (m, 3H), 3.16–2.58 (m, 6H), 2.53–2.39 (m, 2H), 2.03–1.88 (m, 2H), 1.85–1.72 (m, 2H), 1.53–1.39 (m, 2H). ^{13}C NMR (101 MHz, CDCl_3): δ 142.1 (2C), 141.5, 129.1 (2C), 128.4 (2C), 128.3 (2C), 126.6 (2C), 126.0, 82.0 (d, $J = 170.7$ Hz), 64.2 (d, $J = 19.6$ Hz), 60.4, 43.1, 33.5, 33.2 (2C), 32.9 (2C), 32.2. HRMS (ESI) calculated for $\text{C}_{22}\text{H}_{29}\text{FN}$ $[\text{M} + \text{H}]^+$ 326.2279, found 326.2277.

N¹-Phenyl-N²-(6,7,8,9-tetrahydro-5H-benzo[7]annulen-7-yl)-ethane-1,2-diamine (26). A solution of ketone **22** (1.00 equiv, 120 mg, 0.749 mmol) and N¹-phenylethane-1,2-diamine (1.50 equiv, 150 μL , 1.12 mmol) in DCM (29 mL) was stirred for 30 min, followed by the addition of sodium triacetoxyborohydride (2.10 equiv, 333 mg, 1.57 mmol) and subsequent vigorous stirring overnight at rt. The reaction mixture was diluted with sat. aq. NaHCO_3 (30 mL) and was extracted with DCM (3 \times 30 mL). The organic phase was washed with brine (30 mL), dried over anhydrous sodium sulfate, filtered, and concentrated under reduced pressure. The crude was purified by gravity column chromatography (silica gel; Hex/EtOAc 7:3, 1% TEA) to afford compound **26** (187 mg, 0.667 mmol, 89% yield). ^1H NMR (400 MHz, CDCl_3): δ 7.12–7.04 (m, 2H), 7.00 (s, 4H), 6.61 (t, $J = 7.3$ Hz, 1H), 6.56–6.51 (m, 2H), 3.14–3.08 (m, 2H), 2.87–2.80 (m, 2H), 2.75–2.54 (m, 5H), 2.05–1.95 (m, 2H), 1.28–1.19 (m, 2H), signals for the NH are not visible. ^{13}C NMR (101 MHz, CD_3OD): δ 148.6, 142.1 (2C), 130.3 (2C), 130.0 (2C), 127.9 (2C), 119.3, 114.4 (2C), 62.7, 44.7, 41.5, 32.3 (2C), 31.7 (2C). HRMS (ESI) calculated for $\text{C}_{19}\text{H}_{25}\text{N}_2$ $[\text{M} + \text{H}]^+$ 281.2012, found 281.2014.

N-(3-(4-Fluorophenyl)propyl)-6,7,8,9-tetrahydro-5H-benzo[7]annulen-7-amine (**27**). A solution of ketone **22** (1.00 equiv, 100 mg, 0.624 mmol) and 3-(4-fluorophenyl)propan-1-amine (2.00 equiv, 191 mg, 1.25 mmol) in DCM (6.1 mL) was stirred for 30 min before sodium triacetoxyborohydride (2.00 equiv, 265 mg, 1.25 mmol) was added. The reaction mixture was vigorously stirred for 18 h, followed by dilution of the mixture with sat. aq. NaHCO₃ (30 mL) and subsequent extraction with DCM (3 × 30 mL). The combined organic phases were washed with brine (30 mL), dried over anhydrous sodium sulfate, filtered, and concentrated under reduced pressure. The crude was purified with flash chromatography (silica gel; DCM/MeOH 98.5:1.5, 1% TEA) to afford the title compound **27** (150 mg, 0.504 mmol, 81% yield). ¹H NMR (400 MHz, CDCl₃) δ 7.17–7.08 (m, 6H), 7.00–6.93 (m, 2H), 2.88–2.61 (m, 9H), 2.12–2.01 (m, 2H), 1.84–1.73 (m, 2H), 1.35–1.23 (m, 2H), signal for the NH is not visible. ¹³C NMR (101 MHz, CDCl₃): δ 161.4 (d, *J* = 243.8 Hz), 142.7 (2C), 137.9, 129.8 (d, *J* = 8.6 Hz, 2C), 129.0 (2C), 126.3 (2C), 115.2 (d, *J* = 20.4 Hz, 2C), 61.4, 46.6, 34.7 (2C), 33.0, 32.4 (2C), 29.8. HRMS (ESI) calculated for C₂₀H₂₃FN [M + H]⁺ 298.1966, found 298.1969.

N-(3-(4-Fluorophenyl)propyl)-*N*-methyl-6,7,8,9-tetrahydro-5H-benzo[7]annulen-7-amine (**28**). Formic acid (17.0 equiv, 0.5 mL, 13.03 mmol) was added to a solution of **27** (1.00 equiv, 228 mg, 0.767 mmol) in formaldehyde (17.0 equiv, 1.0 mL, 13.03 mmol), which was refluxed at 100 °C for 16 h. The solvent was subsequently evaporated under reduced pressure, diluted with 2 M aq. NaOH (300 mL), and extracted with chloroform (4 × 300 mL). The combined organic layers were washed with brine (500 mL), dried over anhydrous sodium sulfate, filtered, and concentrated under reduced pressure. The resulting crude was purified via flash column chromatography (silica gel; Hex/EtOAc 5:5) to yield compound **28** (118 mg, 0.379 mmol, 49% yield). ¹H NMR (400 MHz, CDCl₃) δ 7.20–7.09 (m, 6H), 7.00–6.91 (m, 2H), 2.84–2.57 (m, 7H), 2.43 (t, *J* = 7.3 Hz, 2H), 2.23 (s, 3H), 2.11–2.01 (m, 2H), 1.76 (p, *J* = 7.3 Hz, 2H), 1.41–1.30 (m, 2H). ¹³C NMR (101 MHz, CDCl₃): δ 161.3 (d, *J* = 242.4 Hz), 142.8 (2C), 138.1, 129.8 (d, *J* = 8.2 Hz, 2C), 129.0 (2C), 126.4 (2C), 115.1 (d, *J* = 21.3 Hz, 2C), 67.9, 53.1, 37.8, 33.6 (2C), 32.9, 30.4, 29.9 (2C). HRMS (ESI) calculated for C₂₁H₂₇FN [M + H]⁺ 312.2122, found 312.2117.

1-(4-Fluorophenyl)-4-(2-nitro-6,7,8,9-tetrahydro-5H-benzo[7]annulen-7-yl)piperazine (**30**). A solution of **29** (1.80 equiv, 150 mg, 0.731 mmol) and 1-(4-fluorophenyl)piperazine (1.00 equiv, 73.0 mg, 0.406 mmol) in DCM (0.4 mL) was stirred for 30 min before sodium triacetoxyborohydride (1.80 equiv, 155 mg, 0.731 mmol) was added to the mixture and subsequently stirred vigorously overnight. The reaction mixture was diluted with sat. aq. NaHCO₃ (30 mL) and extracted with DCM (3 × 30 mL). The combined organic layers were washed using brine (30 mL), dried over anhydrous sodium sulfate, and evaporated under reduced pressure. The resulting crude was purified via flash chromatography (silica gel; DCM/MeOH 100:0, 99:1). The titled compound **30** was then obtained by decanting using MeCN and water (61.0 mg, 0.165 mmol, 41% yield). ¹H NMR (400 MHz, CDCl₃) δ 8.02–7.94 (m, 2H), 7.26 (d, *J* = 8.1 Hz, 1H), 7.00–6.83 (m, 4H), 3.19–2.92 (m, 6H), 2.85–2.59 (m, 7H), 2.24–2.08 (m, 2H), 1.54–1.42 (m, 2H). ¹³C NMR (101 MHz, CDCl₃): δ 157.3 (d, *J* = 238.8 Hz), 150.6, 148.2, 146.6, 144.2, 129.9, 123.9, 121.7, 118.0 (d, *J* = 7.3 Hz, 2C), 115.6 (d, *J* = 21.9 Hz, 2C), 67.6, 51.0 (2C), 48.8 (2C), 33.1, 33.0, 29.8, 29.7. HRMS (ESI) calculated for C₂₁H₂₅FN₃O₂ [M + H]⁺ 370.1925, found 370.1927.

N-Methyl-2-nitro-*N*-(3-phenylpropyl)-6,7,8,9-tetrahydro-5H-benzo[7]annulen-7-amine (**32**). Formic acid (17.0 equiv, 0.3 mL, 8.91 mmol) was added to a solution of **31** (1.00 equiv, 170 mg, 0.524 mmol) in formaldehyde (17.0 equiv, 0.7 mL, 8.91 mmol) and was refluxed at 100 °C for 16 h. The solvent was evaporated under reduced pressure, and the residue was resuspended in 2 M aq. NaOH (300 mL) and extracted with chloroform (4 × 100 mL). Combined organic layers were washed using brine (100 mL), dried over anhydrous sodium sulfate, and concentrated in vacuo. The residue was purified via flash chromatography (silica gel; DCM/MeOH 95:5, 1% NH₃) to afford compound **32** (161 mg, 0.476 mmol, 91% yield).

¹H NMR (400 MHz, CDCl₃) δ 7.99–7.95 (m, 2H), 7.31–7.15 (m, 6H), 2.93 (dd, *J* = 14.4, 7.6 Hz, 2H), 2.78–2.69 (m, 3H), 2.66–2.60 (m, 2H), 2.47–2.41 (m, 2H), 2.22 (s, 3H), 2.14–2.02 (m, 2H), 1.78 (p, *J* = 7.6 Hz, 2H), 1.42–1.30 (m, 2H). ¹³C NMR (101 MHz, CDCl₃): δ 150.7, 146.5, 144.3, 142.5, 129.8, 128.5 (2C), 128.4 (2C), 125.8, 123.8, 121.6, 67.2, 53.2, 37.6, 33.7, 33.5, 33.4, 30.2, 29.6, 29.5. HRMS (ESI) calculated for C₂₁H₂₇N₂O₂ [M + H]⁺ 339.2067, found 339.2070.

4-Fluoro-*N*-(7-oxo-6,7,8,9-tetrahydro-5H-benzo[7]annulen-2-yl)-benzamide (**34**). Amine **33** (1.00 equiv, 160 mg, 0.913 mmol) was dissolved in DCM (1.8 mL) and cooled to 0 °C. TEA (1.00 equiv, 140 μL, 0.913 mmol) was added to the solution, followed by 4-fluorobenzoyl chloride (0.99 equiv, 110 μL, 0.911 mmol) slowly dropwise and was subsequently stirred for 11 h at rt. The mixture was diluted with DCM (25 mL), washed with sat. aq. NaHCO₃ (3 × 10 mL) and then with brine (15 mL), dried over anhydrous sodium sulfate, filtered, and concentrated under reduced pressure. The crude was purified by flash column chromatography (silica gel; Hex/EtOAc 6:4, 1% aq. NH₃) to afford compound **34** (87.0 mg, 0.291 mmol, 32% yield). ¹H NMR (400 MHz, CDCl₃) δ 7.92–7.85 (m, 2H), 7.60 (d, *J* = 2.3 Hz, 1H), 7.40 (dd, *J* = 8.1, 2.3 Hz, 1H), 7.22 (d, *J* = 8.1 Hz, 1H), 7.20–7.15 (m, 2H), 2.95–2.84 (m, 4H), 2.65–2.56 (m, 4H), signal for the NH is not visible. ¹³C NMR (101 MHz, CDCl₃) δ 211.2, 165.1 (d, *J* = 252.4 Hz), 164.8, 141.7, 137.2, 136.8, 130.0 (2C), 129.5 (d, *J* = 9.6 Hz, 2C), 121.2, 118.9, 116.1 (d, *J* = 22.4 Hz, 2C), 44.8, 44.6, 30.9, 30.2. HRMS (ESI) calculated for C₁₈H₁₇FNO₂ [M + H]⁺ 298.1238, found 298.1241.

4-Fluoro-*N*-(7-((3-phenylpropyl)amino)-6,7,8,9-tetrahydro-5H-benzo[7]annulen-2-yl)benzamide (**35**). A solution of **34** (1.00 equiv, 75.0 mg, 0.252 mmol) and 3-phenylpropan-1-amine (2.00 equiv, 72 μL, 0.504 mmol) in DCM (9.0 mL) was stirred for 30 min before sodium triacetoxyborohydride (2.00 equiv, 107 mg, 0.504 mmol) was added and vigorously stirred for 18 h at rt. Sat. aq. NaHCO₃ (100 mL) was added, and the reaction mixture was extracted with DCM (3 × 60 mL). The organic phase was washed with brine (200 mL), dried over anhydrous sodium sulfate, filtered, and concentrated under reduced pressure. The crude was purified by flash column chromatography (silica gel; DCM/MeOH 9:1, 1% aq. NH₃) to afford compound **35** (90.0 mg, 0.215 mmol, 85% yield). ¹H NMR (400 MHz, CDCl₃) δ 7.89–7.80 (m, 2H), 7.43 (d, *J* = 2.1 Hz, 1H), 7.37–7.23 (m, 3H), 7.21–7.15 (m, 3H), 7.14–7.04 (m, 3H), 2.91 (t, *J* = 10.4 Hz, 1H), 2.84–2.70 (m, 4H), 2.70–2.59 (m, 4H), 2.30–2.09 (m, 2H), 1.99 (p, *J* = 7.6 Hz, 2H), 1.49–1.35 (m, 2H), signals for the NH are not visible. ¹³C NMR (101 MHz, CDCl₃) δ 164.9 (d, *J* = 252.7 Hz), 164.7, 143.4, 142.0, 139.2, 135.9 (2C), 131.4, 129.7, 129.5 (d, *J* = 9.1 Hz, 2C), 128.5 (2C), 126.0 (2C), 121.1, 118.1, 115.9 (d, *J* = 22.7 Hz, 2C), 61.4, 46.5, 34.3, 34.2, 33.8 (2C), 32.4, 31.8. HRMS (ESI) calculated for C₂₇H₃₀FN₂O [M + H]⁺ 417.2337, found 417.2344.

N-(7-Oxo-6,7,8,9-tetrahydro-5H-benzo[7]annulen-2-yl)-benzamide (**36**). Amine **33** (1.00 equiv, 160 mg, 0.913 mmol) was dissolved in DCM (1.8 mL) and cooled to 0 °C. TEA (1.00 equiv, 140 μL, 0.913 mmol) was added to the solution, followed by benzoyl chloride (0.99 equiv, 106 μL, 0.911 mmol) slowly dropwise, and the reaction was stirred for 11 h at rt. The mixture was diluted with DCM (25 mL), washed with sat. aq. NaHCO₃ (3 × 10 mL) and then with brine (15 mL), dried over anhydrous sodium sulfate, filtered, and concentrated under reduced pressure. The crude was purified by flash column chromatography (silica gel; Hex/EtOAc 6:4, 1% aq. NH₃) to afford compound **36** (90.0 mg, 0.323 mmol, 35% yield). ¹H NMR (400 MHz, CDCl₃) δ 7.89–7.84 (m, 2H), 7.62 (d, *J* = 2.2 Hz, 1H), 7.58–7.53 (m, 1H), 7.52–7.46 (m, 2H), 7.42 (dd, *J* = 8.1, 2.2 Hz, 1H), 7.24–7.18 (m, 1H), 2.93–2.80 (m, 4H), 2.64–2.52 (m, 4H), signal for the NH is not visible. ¹³C NMR (101 MHz, CDCl₃) δ 211.3, 165.9, 141.6, 137.0, 135.0, 132.6, 132.0, 130.0, 129.0 (2C), 127.1 (2C), 121.2, 118.9, 44.8, 44.6, 30.8, 30.2. HRMS (ESI) calculated for C₁₈H₁₈NO₂ [M + H]⁺ 280.1332, found 280.1333.

N-(7-((3-Phenylpropyl)amino)-6,7,8,9-tetrahydro-5H-benzo[7]annulen-2-yl)benzamide (**37**). A solution of **36** (1.00 equiv, 79.0 mg, 0.281 mmol) and 3-phenylpropan-1-amine (2.00 equiv, 80 μL, 0.562

mmol) in DCM (10 mL) was stirred for 30 min before sodium triacetoxymethylborohydride (2.00 equiv, 119 mg, 0.562 mmol) was added and vigorously stirred for 16 h at rt. Sat. aq. NaHCO_3 (100 mL) was added, and the reaction mixture was extracted with DCM (3×60 mL). The combined organic phases were washed with brine (200 mL), dried over anhydrous sodium sulfate, filtered, and concentrated under reduced pressure. The crude was purified by flash column chromatography (silica gel; DCM/MeOH 9:1, 1% aq. NH_3) to afford compound **37** (80.0 mg, 0.200 mmol, 71% yield). ^1H NMR (400 MHz, CD_3OD) δ 7.94–7.89 (m, 2H), 7.60–7.54 (m, 1H), 7.53–7.47 (m, 2H), 7.46–7.39 (m, 2H), 7.30–7.25 (m, 2H), 7.23–7.14 (m, 3H), 7.10 (d, J = 8.0 Hz, 1H), 2.93–2.64 (m, 9H), 2.24–2.09 (m, 2H), 1.87 (p, J = 7.6 Hz, 2H), 1.34–1.21 (m, 2H), signals for the NH are not visible. ^{13}C NMR (101 MHz, CD_3OD) δ 165.6, 143.9, 139.9, 138.0, 136.4, 132.8, 130.2, 129.6 (2C), 129.5 (2C), 129.4 (2C), 128.6 (2C), 127.0, 122.9, 120.2, 62.8, 47.0, 34.5 (2C), 34.3, 33.3, 32.6, 31.9. HRMS (ESI) calculated for $\text{C}_{27}\text{H}_{31}\text{N}_2\text{O}$ $[\text{M} + \text{H}]^+$ 399.2431, found 399.2432.

N-(7-(3-(4-Fluorophenyl)propyl)amino)-6,7,8,9-tetrahydro-5H-benzo[7]annulen-2-yl)benzamide (**38**). A solution of **36** (1.00 equiv, 9.00 mg, 0.032 mmol) and 3-(4-fluorophenyl)propan-1-amine (2.00 equiv, 10 μL , 0.064 mmol) in DCM (1.2 mL) was stirred for 30 min before sodium triacetoxymethylborohydride (2.00 equiv, 14.0 mg, 0.064 mmol) was added and vigorously stirred for 18 h at rt. Sat. aq. NaHCO_3 (15 mL) was added, and the reaction mixture was extracted with DCM (3×10 mL). The combined organic phases were washed with brine (30 mL), dried over anhydrous sodium sulfate, filtered, and concentrated under reduced pressure. The crude was purified by gravity column chromatography (silica gel; Hex/EtOAc 9:1, 1% aq. NH_3) to afford compound **38** (10.0 mg, 0.023 mmol, 72% yield). ^1H NMR (400 MHz, CD_3OD) δ 7.39–7.34 (m, 2H), 7.32–7.27 (m, 2H), 7.25–7.18 (m, 3H), 7.04–6.98 (m, 2H), 6.83 (d, J = 8.0 Hz, 1H), 6.47 (d, J = 2.4 Hz, 1H), 6.38 (dd, J = 8.0, 2.4 Hz, 1H), 2.89 (tt, J = 10.8, 3.3 Hz, 1H), 2.81–2.75 (m, 2H), 2.71–2.62 (m, 6H), 2.20–2.07 (m, 2H), 1.86 (p, J = 7.6 Hz, 2H), 1.27–1.15 (m, 2H), signals for the NH are not visible. ^{13}C NMR (101 MHz, CDCl_3) δ 166.0, 161.6 (d, J = 244.1 Hz), 142.0, 137.3, 136.8, 136.1, 135.1, 131.9, 129.9 (d, J = 8.3 Hz, 3C), 128.8 (2C), 127.2 (2C), 121.0, 118.4, 115.5 (d, J = 21.9 Hz, 2C), 61.8, 44.6, 32.4 (2C), 32.1 (2C), 31.4, 29.9. HRMS (ESI) calculated for $\text{C}_{27}\text{H}_{30}\text{FN}_2\text{O}$ $[\text{M} + \text{H}]^+$ 417.2337, found 417.2331.

1-(4-Fluorophenyl)-4-(6,7,8,9-tetrahydro-5H-benzo[7]annulen-7-yl)piperazine (**41**). A solution of **40** (1.00 equiv, 235 mg, 0.676 mmol) and 1-(4-fluorophenyl)piperazine (4.90 equiv, 0.6 mL, 3.31 mmol) in MeCN (15 mL) was stirred vigorously for 16 h at 80 $^\circ\text{C}$. The reaction mixture was concentrated in vacuo and purified by gravity column chromatography (silica gel; DCM/MeOH 99:1, 1% NH_3) to afford the title compound **41** (70.0 mg, 0.216 mmol, 32% yield). ^1H NMR (400 MHz, CDCl_3) δ 7.15–7.10 (m, 4H), 7.01–6.82 (m, 4H), 3.17–3.05 (m, 4H), 2.93–2.70 (m, 9H), 2.22–2.08 (m, 2H), 1.53–1.41 (m, 2H). ^{13}C NMR (101 MHz, CDCl_3) δ 157.3 (d, J = 238.6 Hz), 148.3, 142.7 (2C), 129.1, 128.5 (2C), 126.4, 117.9 (d, J = 8.5 Hz, 2C), 115.6 (d, J = 22.1 Hz, 2C), 68.4, 51.0 (2C), 48.7 (2C), 33.4 (2C), 30.2 (2C). HRMS (ESI) calculated for $\text{C}_{21}\text{H}_{26}\text{FN}_2$ $[\text{M} + \text{H}]^+$ 325.2075, found 325.2079.

N-(3-(4-Bromophenyl)propyl)-6,7,8,9-tetrahydro-5H-benzo[7]annulen-7-amine (**42**). A solution of commercially available ketone **22** (1.00 equiv, 371 mg, 2.31 mmol) and 3-(4-bromophenyl)propan-1-amine (2.00 equiv, 710 μL , 4.63 mmol) in DCM (8.2 mL) was stirred for 30 min before sodium triacetoxymethylborohydride (1.50 equiv, 738 mg, 3.48 mmol) was added and vigorously stirred for 16 h at rt. Sat. aq. NaHCO_3 (90 mL) was added, and the reaction mixture was extracted with DCM (3×75 mL). The combined organic phases were washed with brine (180 mL), dried over anhydrous sodium sulfate, filtered, and concentrated under reduced pressure. The crude was purified by flash column chromatography (silica gel; DCM/MeOH 9:1, 1% aq. NH_3) to afford compound **42** (248 mg, 0.691 mmol, 30% yield). ^1H NMR (400 MHz, CDCl_3) δ 7.41–7.36 (m, 2H), 7.13–7.03 (m, 6H), 2.88–2.68 (m, 6H), 2.67–2.58 (m, 3H), 2.21–2.06 (m, 2H), 1.90 (p, J = 7.6 Hz, 2H), 1.37 (q, J = 11.4 Hz,

2H), signal for the NH is not visible. ^{13}C NMR (101 MHz, CDCl_3) δ 142.2, 131.6 (2C), 130.3 (2C), 129.1 (4C), 126.5 (2C), 119.8, 61.5, 45.8, 33.5, 33.0 (2C), 32.3 (2C), 31.0. HRMS (ESI) calculated for $\text{C}_{20}\text{H}_{25}\text{BrN}$ $[\text{M} + \text{H}]^+$ 358.1165, found 358.1167.

Tert-butyl(6,7,8,9-tetrahydro-5H-benzo[7]annulen-7-yl)(3-(4-(4,4,5,5-tetramethyl-1,3,2-dioxaborolan-2-yl)phenyl)propyl)-carbamate (**43**). Compound **42** (1.00 equiv, 236 mg, 0.658 mmol), 4,4,4',4'',5,5',5''-octamethyl-2,2'-bi(1,3,2-dioxaborolane) (1.20 equiv, 201 mg, 0.790 mmol), $\text{PdCl}_2(\text{dppf})$ -DCM Adduct (0.05 equiv, 27.2 mg, 0.033 mmol), and potassium acetate (4.00 equiv, 258 mg, 2.63 mmol) were suspended in DMF (5.8 mL) and stirred at 100 $^\circ\text{C}$ for 5 h. The reaction mixture was then cooled and diluted with water (200 mL) and subsequently extracted with methyl-*tert*-butyl ether (MTBE, 3×60 mL). The combined organic phases were washed with brine (200 mL), dried over anhydrous sodium sulfate, filtered, and concentrated under reduced pressure. The brown crude was dried overnight under high vacuum. The crude (249 mg) was dissolved in MeCN (2.1 mL) before adding di-*tert*-butyl dicarbonate (0.40 mL, 1.84 mmol), *N,N*-dimethylpyridin-4-amine (15.0 mg, 0.123 mmol), and TEA (0.30 mL, 1.84 mmol). The mixture was stirred for 17 h at rt. Afterward, the mixture was concentrated under reduced pressure, and the residue was dissolved in EtOAc (5 mL), washed once with sat. aq. NH_4Cl (5 mL), once with water (5 mL), and then once with brine (5 mL). The organic phase was then dried over anhydrous sodium sulfate, filtered, and concentrated under reduced pressure. The crude was purified by flash column chromatography (silica gel; Hex/EtOAc 9:1) to afford compound **43** (293 mg, 0.579 mmol, 34% yield). ^1H NMR (400 MHz, CDCl_3) δ 7.70 (d, J = 7.9 Hz, 2H), 7.16–7.08 (m, 6H), 4.34–4.18 (m, 1H), 3.04 (d, J = 52.9 Hz, 2H), 2.87–2.66 (m, 4H), 2.52 (t, J = 7.6 Hz, 2H), 2.03–1.92 (m, 2H), 1.80 (p, J = 7.6 Hz, 2H), 1.45 (s, 9H), 1.33 (s, 12H), 1.29–1.23 (m, 2H). ^{13}C NMR (101 MHz, CDCl_3) δ 155.3, 145.6, 142.3, 135.1 (2C), 129.1 (4C), 127.8 (2C), 126.6 (2C), 83.8, 79.5 (2C), 64.2, 43.2, 34.0 (2C), 33.4 (2C), 33.2, 32.4, 28.7 (3C), 25.0 (4C). HRMS (ESI) calculated for $\text{C}_{31}\text{H}_{45}\text{BNO}_4$ $[\text{M} + \text{H}]^+$ 506.3442, found 506.3454.

3-(4-(4-Iodophenyl)butyl)-7-methoxy-2,3,4,5-tetrahydro-1H-benzo[d]azepin-1-ol (**46**). TEA (1.80 equiv, 4.00 mL, 28.6 mmol) was added to a solution of **45** (1.00 equiv, 4.39 g, 15.9 mmol) dissolved in DCM (160 mL). Under cooling with ice, MsCl (1.03 equiv, 1.30 mL, 16.5 mmol) was added dropwise. After 5 min of stirring, the reaction mixture was allowed to come to rt, and stirring was continued for 30 min. The reaction mixture was quenched with water (200 mL) and extracted with DCM (3×200 mL). The combined organic layers were washed with brine, dried over anhydrous sodium sulfate, filtered, and concentrated under reduced pressure. The resulting residue and **12** (350 mg, 1.81 mmol) were dissolved in DMF (18 mL) before the dropwise addition of *N,N*-diisopropylethylamine (276 μL , 1.58 mmol). The reaction mixture was refluxed at 90 $^\circ\text{C}$ for 2.5 h before the mixture was diluted with 1 mM aq. NaOH (400 mL) and extracted with DCM (3×300 mL). The combined organic layers were washed with brine (500 mL), dried over anhydrous sodium sulfate, filtered, and concentrated under reduced pressure. The crude was purified by flash column chromatography (silica gel; Hex/EtOAc 8:2 to 2:8, 0.1% aq. NH_3), resulting in the title compound **46** (459 mg, 1.08 mmol, 56% yield). ^1H NMR (400 MHz, CDCl_3) δ 7.63–7.55 (m, 2H), 7.10 (d, J = 8.0 Hz, 1H), 6.98–6.90 (m, 2H), 6.72–6.59 (m, 2H), 4.57 (d, J = 6.7 Hz, 1H), 3.78 (s, 3H), 3.32–3.21 (m, 1H), 3.19–3.09 (m, 1H), 3.03–2.94 (m, 1H), 2.65 (dd, J = 15.2, 5.9 Hz, 1H), 2.59 (t, J = 7.2 Hz, 4H), 2.50 (d, J = 11.7 Hz, 1H), 2.40 (t, J = 11.7 Hz, 1H), 1.66–1.51 (m, 4H), signal for OH is not visible. ^{13}C NMR (101 MHz, CDCl_3) δ 159.1, 142.0, 141.3, 137.5 (2C), 135.7, 130.7 (2C), 129.9, 116.7, 110.3, 90.9, 72.6, 60.9, 59.7, 56.3, 55.3, 37.0, 35.4, 29.0, 26.7. HRMS (ESI) calculated for $\text{C}_{21}\text{H}_{27}\text{INO}_2$ $[\text{M} + \text{H}]^+$ 452.1081, found 452.1083.

3-(4-(2-Bromophenyl)butyl)-7-methoxy-2,3,4,5-tetrahydro-1H-benzo[d]azepin-1-yl Acetate (**47**). Hydroxyl **46** (1.00 equiv, 455 mg, 1.01 mmol) and DMAP (0.22 equiv, 27.0 mg, 0.222 mmol) were dissolved in DCM (25 mL), before the dropwise addition of TEA

(4.10 equiv, 0.60 mL, 4.15 mmol) and acetic anhydride (2.00 equiv, 0.20 mL, 2.02 mmol). After stirring at rt overnight, the reaction mixture was diluted with sat. aq. NaHCO_3 (50 mL) and extracted with DCM (3×75 mL). The combined organic layers were washed with brine (180 mL), dried over anhydrous sodium sulfate, filtered, and concentrated under reduced pressure. The crude was purified by flash column chromatography (silica gel; Hex/EtOAc 7:3, 0.1% aq. NH_3) affording **47** (341 mg, 0.692 mmol, 69% yield). ^1H NMR (400 MHz, CDCl_3) δ 7.65–7.48 (m, 2H), 7.18 (d, J = 8.2 Hz, 1H), 6.97–6.86 (m, 2H), 6.76–6.60 (m, 2H), 5.90–5.81 (m, 1H), 3.79 (s, 3H), 3.10 (dd, J = 14.1, 9.4 Hz, 1H), 2.96 (dd, J = 12.6, 7.5 Hz, 1H), 2.88–2.77 (m, 1H), 2.76–2.60 (m, 3H), 2.55 (q, J = 8.5, 7.9 Hz, 4H), 2.12 (s, 3H), 1.66–1.56 (m, 2H), 1.55–1.43 (m, 2H). ^{13}C NMR (101 MHz, CDCl_3) δ 170.3, 159.3, 142.3, 137.4 (3C), 131.5, 130.7 (2C), 128.6, 116.0, 110.5, 90.8, 75.0, 58.4 (2C), 55.3, 55.2, 36.0, 35.4, 29.1, 26.5, 21.5. HRMS (ESI) calculated for $\text{C}_{23}\text{H}_{29}\text{INO}_3$ [$\text{M} + \text{H}$] $^+$ 494.1187, found 494.1179.

7-Methoxy-3-(4-(4-(4,4,5,5-tetramethyl-1,3,2-dioxaborolan-2-yl)phenyl)butyl)-2,3,4,5-tetrahydro-1H-benzo[d]azepin-1-yl Acetate (48). Compound **47** (1.00 equiv, 310 mg, 0.628 mmol), 4,4',4'',5,5',5''-octamethyl-2,2'-bi(1,3,2-dioxaborolane) (1.20 equiv, 197 mg, 0.777 mmol), potassium acetate (4.00 equiv, 246 mg, 2.51 mmol), and $\text{PdCl}_2(\text{dppf})$ -DCM adduct (0.05 equiv, 27.2 mg, 0.033 mmol) were dissolved in DMF (7.2 mL) and stirred under reflux at 100 °C for 5 h before the reaction mixture was diluted with water (100 mL) and extracted with MTBE (3×225 mL). The combined organic layers were washed with brine (600 mL), dried over anhydrous sodium sulfate, filtered, and concentrated under reduced pressure. The crude was purified by flash column chromatography (silica gel; Hex/EtOAc 7:3, 0.1% aq. NH_3) affording **48** (246 mg, 0.499 mmol, 79% yield). ^1H NMR (400 MHz, CDCl_3) δ 7.72 (d, J = 8.0 Hz, 2H), 7.18 (dd, J = 8.0, 6.2 Hz, 3H), 6.74–6.59 (m, 2H), 5.86 (d, J = 6.4 Hz, 1H), 3.78 (s, 3H), 3.10 (dd, J = 14.1, 8.9 Hz, 1H), 2.97 (dd, J = 12.6, 7.4 Hz, 1H), 2.81 (dd, J = 14.5, 7.9 Hz, 1H), 2.72–2.59 (m, 5H), 2.58–2.52 (m, 2H), 2.11 (s, 3H), 1.63 (p, J = 7.2 Hz, 2H), 1.56–1.45 (m, 2H), 1.34 (s, 12H). ^{13}C NMR (101 MHz, CDCl_3) δ 170.3, 159.3, 146.1, 142.4, 135.0 (2C), 131.5, 128.7 (2C), 128.0, 115.9, 110.5, 83.7 (2C), 75.1, 60.5, 58.6, 58.5, 55.3, 55.2, 36.1, 36.0, 29.2, 26.6, 25.0 (4C), 21.5. HRMS (ESI) calculated for $\text{C}_{29}\text{H}_{41}\text{BNO}_5$ [$\text{M} + \text{H}$] $^+$ 494.3077, found 494.3082.

In Vitro Binding Assay. The binding assay for GluN2B containing NMDARs followed previously published procedures.^{38,57} In brief, mouse L(tk $^-$) cells carrying the stably transfected dexamethasone-inducible eukaryotic expression vectors pMSG NR1a and pMSG NR2B in a 1:5 ratio were employed. The competitive binding assay was performed with the radioligand [^3H]ifenprodil (60 Ci/mmol, PerkinElmer) using standard 96-well multiplates (Diagonal, Muenster, Germany). For the affinity determination toward $\sigma 1$ and $\sigma 2$ receptors, a previously published and well-established binding assay was used.^{58–60} The radioligands used were [^3H](+)-pentazocine and [^3H]di-o-tolylguanidine for $\sigma 1$ and $\sigma 2$ receptor binding assays, respectively. Triplicate measurements are reported with standard error of measurement (SEM). Alternatively, whole rat brain membranes were used for IC_{50} testing of the compounds for the determination of the affinity toward $\sigma 1\text{Rs}$ as previously reported.⁶¹ The whole brain rat membranes were prepared as previously described.⁶² For determination of IC_{50} toward GluN2B subunit-containing NMDARs, a dilution series of 8 different concentrations of the compounds in question was prepared, ranging from 30 pM to 30 μM . [^3H]ifenprodil was added to the different dilutions of the test ligand together with brain membranes (1 mg/mL total protein concentration) in HEPES buffer (30 mM 4-(2-hydroxyethyl)piperazine-1-ethanesulfonic acid sodium salt (HEPES), 110 mM NaCl, 5 mM KCl, 2.5 mM CaCl_2 , 1.2 mM MgCl_2 , pH 7.4) in a total volume of 200 μL . Nonspecific binding was determined in the presence of CP-101,606, while total binding was attained in the exclusive presence of buffer and brain membranes. The test samples were incubated at 25 °C for 60 min under mechanical shaking (110 rpm). Termination of the incubation and removal of the free radioligand were achieved by the further addition of 3 mL of

HEPES buffer, followed by vacuum filtration through glass microfiber filter paper (Whatman, GF/C 25 mm, preincubated in 0.05% polyethylenimine for 30 min). Afterward, scintillation fluid (10 mL/scintillation vial, Ultima Gold, Perkin-Elmer) was added to the filters, and the activity was measured by a Packard 2200CA TRI-CARB liquid scintillation analyzer.

Radiochemistry. [^{18}F]fluoride ions were produced by bombardment of 98% enriched ^{18}O -water via the $e^{-18}\text{O}(\text{p,n})^{18}\text{F}$ nuclear reaction using a Cyclone 18/9 cyclotron (18-MeV; IBA Belgium). Aqueous [^{18}F]fluoride was trapped on a preconditioned anion-exchange cartridge (Waters SepPak Accell QMA cartridge carbonate) and then eluted with a solution of kryptofix 2.2.2 (6.3 mg/mL), $\text{K}_2\text{C}_2\text{O}_4$ (1 mg/mL), and K_2CO_3 (0.1 mg/mL) in MeCN/ H_2O (4:1, 0.9 mL), followed by azeotropic drying with MeCN (3×0.8 mL).⁵³ The reaction vial was purged with air (20 mL), and the residue was redissolved in a solution of 6–8 mg of boronic ester precursor, either **45** or **48**, and 14 mg of $\text{Cu}(\text{OTf})_2(\text{py})_4$ in 0.3 mL of dry dimethylacetamide (DMA). The resulting solution was stirred at 120 °C for 20 min.

The Boc-protected [^{18}F]**49** crude was diluted with 2 mL of water/MeCN (1:1) and then treated with 0.7 mL of 7 M HCl for 10 min at 95 °C. The formed [^{18}F]**27** was purified via semipreparative HPLC. The collected fractions were diluted with 35 mL of water and trapped on a C18 Light cartridge (Waters, preconditioned with 5 mL of EtOH and 5 mL of water). The cartridge was washed with water (5 mL), followed by product elution with 0.5 mL of EtOH into the final formulation vial. Finally, the product was formulated with 5% EtOH in water for injection.

For the acetyl-protected [^{18}F]**50**, the reaction mixture was diluted with 35 mL of water, before trapping the intermediate on a C18 Plus cartridge (Waters, preconditioned with 5 mL of MeCN and 5 mL of water). After washing the cartridge with water (5 mL), the product was eluted with 2 mL of EtOH. The solvent was evaporated at 95 °C for 5 min, followed by azeotropic drying with MeCN ($3 \text{ mL} \times 0.8 \text{ mL}$). The residue was cooled down in an ice bath before redissolving it in 0.4 mL of DCM. The vial was kept in an ice bath, and 1 mL of BBr_3 (1 M in DCM) was added simultaneously, followed by stirring at rt for 15 min. The DCM was evaporated, and the crude was then redissolved in aq. 0.1% $\text{H}_3\text{PO}_4/\text{MeCN}$ (5:1, 3 mL). Subsequently, the product was purified by semipreparative HPLC. Collected fractions were diluted with 35 mL of water, and the product was trapped on a C18 Light cartridge (Waters, preconditioned with 5 mL of EtOH and 5 mL of water). The cartridge was washed with 5 mL of water, followed by product elution with 0.5 mL of absolute EtOH. The product was formulated with 5% EtOH in WFI to afford [^{18}F]PF-NB1. Enantiomeric purity was not tested post radiosynthesis for (R)- and (S)- [^{18}F]PF-NB1.

In Vitro Autoradiography. Adult rat or mouse brain tissues embedded in optimum cutting temperature medium were prepared as 10 μm -thick coronal sections on a cryostat (Cryo-Star HM 560 MV; Microm, Thermo Scientific, Wilmington, DE). Slices were adsorbed on SuperFrost Plus glass slides (Menzel, Braunschweig, Germany) and subsequently stored at -20 °C. At the start of autoradiography, slices were thawed for 15 min on ice and subsequently preconditioned in an aqueous buffer comprising 30 mM HEPES, 0.56 mM MgCl_2 , 110 mM NaCl, 5 mM KCl, 3.3 mM CaCl_2 , and 0.1% fatty acid free bovine serum albumin (pH 7.4, 0 °C) for 10 min. The slides were left to dry for 2–3 min at rt and then incubated with 2.9–3.1 nM of (R)-[^{18}F]PF-NB1, (S)-[^{18}F]PF-NB1, [^{18}F]PF-NB1, or [^{18}F]**27** for 20 min at rt in a humidified chamber. For blockade experiments, 1 μM of GluN2B ligands, CERC-301 (IC_{50} for GluN2B = 3.6 nM⁶³) and CP-101,606 (IC_{50} for GluN2B = 11 nM⁵⁴), was used. For the negative control, 1 μM of $\sigma 1\text{R}$ ligands, SA4503 (IC_{50} for $\sigma 1\text{R}$ = 17.4 nM⁶⁴) and fluspidine (K_i for $\sigma 1\text{R}$ = 0.59 nM⁶⁵), as well as the $\sigma 2\text{R}$ blocker PB28 (K_i $\sigma 1\text{R}$ = 0.68 nM⁶⁶), was used. The slices were decanted and washed for 5 min in an aqueous buffer containing 30 mM HEPES, 0.56 mM MgCl_2 , 110 mM NaCl, 5 mM KCl, 3.3 mM CaCl_2 , and 0.1% fatty acid free bovine serum albumin (pH 7.4, 0 °C). Subsequently, the slices were washed (2×3 min) in an aqueous buffer containing 30 mM HEPES, 0.56 mM MgCl_2 , 110 mM NaCl, 5 mM KCl, 3.3 mM

CaCl₂ (pH 7.4), and (2 × 5 s) in distilled water. After drying the slices for 5 min at rt, they were exposed to a phosphor imager plate (Fuji, Dielsdorf, Switzerland) for 35–40 min. The films were scanned by a BAS5000 reader (Fuji), and data analysis was performed using AIDA 4.50.010 software (Raytest Isotopenmessgeräte GmbH, Straubenhardt, Germany).

In Vivo PET Imaging. Animal care and experiments were compliant with Swiss Animal Welfare legislation and were authorized by the Veterinary Office of the Canton Zurich, Zurich, Switzerland. Wistar male rats were purchased from Charles River (Sulzfeld, Germany), while CD1 and σ 1R-KO mice were purchased from Envigo (Barcelona, Spain). Wistar rats (317–423 g) and mice (40.5–44.1 g) were anesthetized using isoflurane and scanned inside a PET/CT scanner (Super Argus, Sedecal, Madrid, Spain) upon tail-vein injection of 30.13–34.68 MBq, 0.7–1.1 nmol/kg (rats, scan time 0–90 min postinjection), or 12.11–14.87 MBq, 1.99–3.80 nmol/kg (mice, scan time 1–91 min postinjection), of [¹⁸F]PF-NB1. For anatomical alignment, PET scans were followed by computed tomography (CT). For blockade studies, escalating doses of CP-101,606 (1, 3, 5 and 10 mg/kg) were injected into Wistar rats 1 min prior to tracer injection. The resulting data were reconstructed in user-defined time frames with a voxel size of 0.3875 × 0.3875 × 0.775 mm³³ as previously detailed by our group.³³ Time–activity curves for specific brain regions of interest were defined on an MRI T2 template by PMOD v3.9 (PMOD Technologies, Zurich, Switzerland). The results are given as standardized uptake values (SUVs), which is the decay-corrected tissue radioactivity normalized to the injected radioactivity and body weight.

Metabolite Study. Wistar rats were injected with 72.8–436 MBq (0.95–14.75 nmol/kg) of [¹⁸F]PF-NB1. Brain homogenate extracts at predefined times (15, 30, and 60 min) and blood (5, 15, 30, 45, 60 min) were acquired and evaluated by radio-ultraperformance liquid chromatography (UPLC).

Biodistribution Study. Eight male Wistar rats (4 baseline and 4 blockade animals) were injected with [¹⁸F]PF-NB1 via tail-vein injection (20.0–26.9 MBq, 0.33–0.57 nmol/kg) and sacrificed by decapitation under anesthesia using isoflurane at 45 min postinjection. For blockade experiments, 2 mg/kg eliprodil in a vehicle of aqueous glucose (5%), NaCl (0.45%), and citric acid (1 mM) was injected momentarily prior to tracer injection. Organs were separated and weighed and radioactivity was measured in a γ -counter (Perkin-Elmer, Schwerzenbach, Switzerland). Biodistribution results are reported in the Supporting Information section as % normalized injected dose/gram tissue. For statistical analysis, an independent two-tailed paired Student's test assuming a normal distribution of the data set was employed to determine statistical probability values.

■ ASSOCIATED CONTENT

● Supporting Information

The Supporting Information is available free of charge on the ACS Publications website at DOI: 10.1021/acs.jmedchem.9b00812.

General procedures; circular dichroism (CD) spectra of (S)/(R)-PF-NB1 and -Me-NB1; time–activity curves (TACs) of [¹⁸F]PF-NB1 in different brain regions of interest; ex vivo metabolite study of [¹⁸F]PF-NB1 in rat brain up to 60 min; brain and body biodistribution studies of [¹⁸F]PF-NB1; calibration curve of PF-NB1 for molar activity calculation; references (PDF)

Molecular formula strings (CSV)

■ AUTHOR INFORMATION

Corresponding Author

*E-mail: simon.ametamey@pharma.ethz.ch.

ORCID

Hazem Ahmed: 0000-0001-7047-5202

Ahmed Haider: 0000-0002-5204-4473

Bernhard Wünsch: 0000-0002-9030-8417

Simon M. Ametamey: 0000-0003-4285-6731

Author Contributions

^{||}H.A. and A.H. contributed equally.

Notes

The authors declare no competing financial interest.

■ ACKNOWLEDGMENTS

This project was supported by the Swiss National Science Foundation Grant Nos. 310030E-160403/1 and 310030E_182872/1. The Table of Contents (TOC) graphic was constructed using biorender.com. Dr. Jose Miguel Vela is acknowledged for providing our group with the σ 1R-KO mice.

■ ABBREVIATIONS

NMDARs, N-methyl-D-aspartate receptors; σ Rs, sigma receptors; BBr₃, boron tribromide; HCl, hydrochloric acid; KF, potassium fluoride; CsF, cesium fluoride; KOAc, potassium acetate; RCY, radiochemical yield; EOB, end of bombardment; MeCN, acetonitrile; SUV, standardized uptake value; Bq, becquerel; TACs, time–activity curves; RO, receptor occupancy; KO, knockout; EtOAc, ethyl acetate; EtOH, ethanol; NH₄HCO₃, ammonium hydrogen carbonate; H₃PO₄, phosphoric acid; K₂CO₃, potassium carbonate; CDCl₃, deuterated chloroform; Hex, hexane; MeOH, methanol; NaOH, sodium hydroxide

■ REFERENCES

- (1) Traynelis, S. F.; Wollmuth, L. P.; McBain, C. J.; Menniti, F. S.; Vance, K. M.; Ogden, K. K.; Hansen, K. B.; Yuan, H.; Myers, S. J.; Dingledine, R. Glutamate receptor ion channels: structure, regulation, and function. *Pharmacol. Rev.* **2010**, *62*, 405–496.
- (2) Furukawa, H.; Singh, S. K.; Mancusso, R.; Gouaux, E. Subunit arrangement and function in NMDA receptors. *Nature* **2005**, *438*, 185–192.
- (3) Paoletti, P.; Bellone, C.; Zhou, Q. NMDA receptor subunit diversity: impact on receptor properties, synaptic plasticity and disease. *Nat. Rev. Neurosci.* **2013**, *14*, 383–400.
- (4) Iacobucci, G. J.; Popescu, G. K. NMDA receptors: linking physiological output to biophysical operation. *Nat. Rev. Neurosci.* **2017**, *18*, 236–249.
- (5) Mony, L.; Kew, J. N.; Gunthorpe, M. J.; Paoletti, P. Allosteric modulators of NR2B-containing NMDA receptors: molecular mechanisms and therapeutic potential. *Br. J. Pharmacol.* **2009**, *157*, 1301–1317.
- (6) Zhou, X.; Hollern, D.; Liao, J.; Andrechek, E.; Wang, H. NMDA receptor-mediated excitotoxicity depends on the coactivation of synaptic and extrasynaptic receptors. *Cell Death Dis.* **2013**, *4*, No. e560.
- (7) Carvajal, F. J.; Mattison, H. A.; Cerpa, W. Role of NMDA Receptor-Mediated Glutamatergic Signaling in Chronic and Acute Neuropathologies. *Neural Plast.* **2016**, *2016*, No. 2701526.
- (8) Olivares, D.; Deshpande, V. K.; Shi, Y.; Lahiri, D. K.; Greig, N. H.; Rogers, J. T.; Huang, X. N-methyl D-aspartate (NMDA) receptor antagonists and memantine treatment for Alzheimer's disease, vascular dementia and Parkinson's disease. *Curr. Alzheimer Res.* **2012**, *9*, 746–758.
- (9) Hynd, M. R.; Scott, H. L.; Dodd, P. R. Glutamate-mediated excitotoxicity and neurodegeneration in Alzheimer's disease. *Neurochem. Int.* **2004**, *45*, 583–595.
- (10) Hardingham, G. E.; Bading, H. Synaptic versus extrasynaptic NMDA receptor signalling: implications for neurodegenerative disorders. *Nat. Rev. Neurosci.* **2010**, *11*, 682–696.

- (11) Kemp, J. A.; Kew, J. N. C.; Gill, R. NMDA Receptor Antagonists and Their Potential as Neuroprotective Agents. In *Ionotropic Glutamate Receptors in the CNS*; Jonas, P.; Monyer, H., Eds.; Springer Berlin Heidelberg: Berlin, Heidelberg, 1999; pp 495–527.
- (12) Nutt, J. G.; Gunzler, S. A.; Kirchhoff, T.; Hogarth, P.; Weaver, J. L.; Krams, M.; Jamerson, B.; Menniti, F. S.; Landen, J. W. Effects of a NR2B selective NMDA glutamate antagonist, CP-101,606, on dyskinesia and Parkinsonism. *Mov. Disord.* **2008**, *23*, 1860–1866.
- (13) Di, X.; Bullock, R.; Watson, J.; Fatouros, P.; Chenard, B.; White, F.; Corwin, F. Effect of CP101,606, a novel NR2B subunit antagonist of the N-methyl-D-aspartate receptor, on the volume of ischemic brain damage off cytotoxic brain edema after middle cerebral artery occlusion in the feline brain. *Stroke* **1997**, *28*, 2244–2251.
- (14) Taniguchi, K.; Shinjo, K.; Mizutani, M.; Shimada, K.; Ishikawa, T.; Menniti, F. S.; Nagahisa, A. Antinociceptive activity of CP-101,606, an NMDA receptor NR2B subunit antagonist. *Br. J. Pharmacol.* **1997**, *122*, 809–812.
- (15) Steece-Collier, K.; Chambers, L. K.; Jaw-Tsai, S. S.; Menniti, F. S.; Greenamyre, J. T. Antiparkinsonian actions of CP-101,606, an antagonist of NR2B subunit-containing N-methyl-D-aspartate receptors. *Exp. Neurol.* **2000**, *163*, 239–243.
- (16) Nash, J. E.; Ravenscroft, P.; McGuire, S.; Crossman, A. R.; Menniti, F. S.; Brotchie, J. M. The NR2B-selective NMDA receptor antagonist CP-101,606 exacerbates L-DOPA-induced dyskinesia and provides mild potentiation of anti-parkinsonian effects of L-DOPA in the MPTP-lesioned marmoset model of Parkinson's disease. *Exp. Neurol.* **2004**, *188*, 471–479.
- (17) Miller, O. H.; Yang, L.; Wang, C. C.; Hargroder, E. A.; Zhang, Y.; Delpire, E.; Hall, B. J. GluN2B-containing NMDA receptors regulate depression-like behavior and are critical for the rapid antidepressant actions of ketamine. *eLife* **2014**, *3*, No. e03581.
- (18) Layer, R. T.; Popik, P.; Olds, T.; Skolnick, P. Antidepressant-like actions of the polyamine site NMDA antagonist, eliprodil (SL-82.0715). *Pharmacol., Biochem. Behav.* **1995**, *52*, 621–627.
- (19) Buckner, R. L. The cerebellum and cognitive function: 25 years of insight from anatomy and neuroimaging. *Neuron* **2013**, *80*, 807–815.
- (20) Kemp, J. A.; McKernan, R. M. NMDA receptor pathways as drug targets. *Nat. Neurosci.* **2002**, *5*, 1039–1042.
- (21) Williams, K. Ifenprodil, a novel NMDA receptor antagonist: site and mechanism of action. *Curr. Drug Targets* **2001**, *2*, 285–298.
- (22) Falck, E.; Begrow, F.; Verspohl, E.; Wunsch, B. Metabolism studies of ifenprodil, a potent GluN2B receptor antagonist. *J. Pharm. Biomed. Anal.* **2014**, *88*, 96–105.
- (23) Karakas, E.; Simorowski, N.; Furukawa, H. Subunit arrangement and phenylethanolamine binding in GluN1/GluN2B NMDA receptors. *Nature* **2011**, *475*, 249–253.
- (24) Contreras, P. C.; Bremer, M. E.; Gray, N. M. Ifenprodil and SL 82.0715 potentially inhibit binding of [3H](+)-3-PPP to sigma binding sites in rat brain. *Neurosci. Lett.* **1990**, *116*, 190–193.
- (25) Maurice, T.; Su, T. P. The pharmacology of sigma-1 receptors. *Pharmacol. Ther.* **2009**, *124*, 195–206.
- (26) Tajima, N.; Karakas, E.; Grant, T.; Simorowski, N.; Diaz-Avalos, R.; Grigorieff, N.; Furukawa, H. Activation of NMDA receptors and the mechanism of inhibition by ifenprodil. *Nature* **2016**, *534*, 63–68.
- (27) Addy, C.; Assaid, C.; Hreniuk, D.; Stroh, M.; Xu, Y.; Herring, W. J.; Ellenbogen, A.; Jinnah, H. A.; Kirby, L.; Leibowitz, M. T.; Stewart, R. M.; Tarsy, D.; Tetrad, J.; Stoch, S. A.; Gottesdiener, K.; Wagner, J. Single-dose administration of MK-0657, an NR2B-selective NMDA antagonist, does not result in clinically meaningful improvement in motor function in patients with moderate Parkinson's disease. *J. Clin. Pharmacol.* **2009**, *49*, 856–864.
- (28) Herring, W. J.; Assaid, C.; Budd, K.; Vargo, R.; Mazenko, R. S.; Lines, C.; Ellenbogen, A.; Verhagen Metman, L. A Phase Ib Randomized Controlled Study to Evaluate the Effectiveness of a Single-Dose of the NR2B Selective N-Methyl-D-Aspartate Antagonist MK-0657 on Levodopa-Induced Dyskinesias and Motor Symptoms in Patients With Parkinson Disease. *Clin. Neuropharmacol.* **2017**, *40*, 255–260.
- (29) Simon, G. M.; Niphakis, M. J.; Cravatt, B. F. Determining target engagement in living systems. *Nat. Chem. Biol.* **2013**, *9*, 200–205.
- (30) Takano, A.; Varrone, A.; Gulyas, B.; Salvadori, P.; Gee, A.; Windhorst, A.; Vercouillie, J.; Bormans, G.; Lammertsma, A. A.; Halldin, C. Guidelines to PET measurements of the target occupancy in the brain for drug development. *Eur. J. Nucl. Med. Mol. Imaging* **2016**, *43*, 2255–2262.
- (31) Haider, A.; Muller Herder, A.; Kramer, S. D.; Varisco, J.; Keller, C.; Frauenknecht, K.; Auberson, Y. P.; Temme, L.; Robaa, D.; Sippl, W.; Schibli, R.; Wunsch, B.; Mu, L.; Ametamey, S. M. Preclinical Evaluation of Benzazepine-Based PET Radioligands (R)- and (S)-(11)C-Me-NB1 Reveals Distinct Enantiomeric Binding Patterns and Tightrope Walk between GluN2B- and Sigma1 Receptor-Targeted PET Imaging. *J. Nucl. Med.* **2019**, *60*, 1167–1173.
- (32) Tewes, B.; Frehland, B.; Schepmann, D.; Schmidtke, K. U.; Winckler, T.; Wunsch, B. Design, Synthesis, and Biological Evaluation of 3-Benzazepin-1-ols as NR2B-Selective NMDA Receptor Antagonists. *ChemMedChem* **2010**, *5*, 687–695.
- (33) Krämer, S. D.; Betzel, T.; Mu, L.; Haider, A.; Herde, A. M.; Boninsegni, A. K.; Keller, C.; Szermerski, M.; Schibli, R.; Wunsch, B.; Ametamey, S. M. Evaluation of (11)C-Me-NB1 as a Potential PET Radioligand for Measuring GluN2B-Containing NMDA Receptors, Drug Occupancy, and Receptor Cross Talk. *J. Nucl. Med.* **2018**, *59*, 698–703.
- (34) Fuchigami, T.; Nakayama, M.; Yoshida, S. Development of PET and SPECT probes for glutamate receptors. *Sci. World J.* **2015**, No. 716514.
- (35) Moses, W. W. Fundamental limits of spatial resolution in PET. *Nucl. Instrum. Methods Phys. Res., Sect. A* **2011**, *648*, S236–S240.
- (36) Haider, A.; Iten, I.; Ahmed, H.; Muller Herder, A.; Gruber, S.; Kramer, S. D.; Keller, C.; Schibli, R.; Wunsch, B.; Mu, L.; Ametamey, S. M. Identification and Preclinical Evaluation of a Radiofluorinated Benzazepine Derivative for Imaging the GluN2B Subunit of the Ionotropic NMDA Receptor. *J. Nucl. Med.* **2019**, *60*, 259–266.
- (37) Börgel, F.; Szermerski, M.; Schreiber, J. A.; Temme, L.; Strutz-Seebohm, N.; Lehmkuhl, K.; Schepmann, D.; Ametamey, S. M.; Seebohm, G.; Schmidt, T. J.; Wunsch, B. Synthesis and Pharmacological Evaluation of Enantiomerically Pure GluN2B Selective NMDA Receptor Antagonists. *ChemMedChem* **2018**, *13*, 1580–1587.
- (38) Benner, A.; Bonifazi, A.; Shirataki, C.; Temme, L.; Schepmann, D.; Quaglia, W.; Shoji, O.; Watanabe, Y.; Daniliuc, C.; Wunsch, B. GluN2B-selective N-methyl-D-aspartate (NMDA) receptor antagonists derived from 3-benzazepines: synthesis and pharmacological evaluation of benzo[7]annulen-7-amines. *ChemMedChem* **2014**, *9*, 741–751.
- (39) Borza, I.; Domany, G. NR2B selective NMDA antagonists: the evolution of the ifenprodil-type pharmacophore. *Curr. Top. Med. Chem.* **2006**, *6*, 687–695.
- (40) Dey, S.; Temme, L.; Schreiber, J. A.; Schepmann, D.; Frehland, B.; Lehmkuhl, K.; Strutz-Seebohm, N.; Seebohm, G.; Wunsch, B. Deconstruction – reconstruction approach to analyze the essential structural elements of tetrahydro-3-benzazepine-based antagonists of GluN2B subunit containing NMDA receptors. *Eur. J. Med. Chem.* **2017**, *138*, S52–S54.
- (41) Tewes, B.; Frehland, B.; Schepmann, D.; Schmidtke, K. U.; Winckler, T.; Wunsch, B. Conformationally constrained NR2B selective NMDA receptor antagonists derived from ifenprodil: Synthesis and biological evaluation of tetrahydro-3-benzazepine-1,7-diols. *Bioorg. Med. Chem.* **2010**, *18*, 8005–8015.
- (42) Jefferies, L. R.; Cook, S. P. Iron-catalyzed arene alkylation reactions with unactivated secondary alcohols. *Org. Lett.* **2014**, *16*, 2026–2029.
- (43) Siddiqui, B. S.; Firdous; Begum, S. A new reagent for the methylation of carboxyl groups. *Tetrahedron Lett.* **2001**, *42*, 9059–9060.

- (44) Pingali, H.; Jain, M.; Shah, S.; Basu, S.; Makadia, P.; Goswami, A.; Zaware, P.; Patil, P.; Godha, A.; Giri, S.; Goel, A.; Patel, M.; Patel, H.; Patel, P. Discovery of a highly orally bioavailable *c*-5-[6-(4-Methanesulfonyloxyphenyl)hexyl]-2-methyl-1,3-dioxane-*r*-2-carboxylic acid as a potent hypoglycemic and hypolipidemic agent. *Bioorg. Med. Chem. Lett.* **2008**, *18*, 5586–5590.
- (45) Gawaskar, S.; Schepmann, D.; Bonifazi, A.; Wünsch, B. Synthesis, GluN2B affinity and selectivity of benzo[7]annulen-7-amines. *Bioorg. Med. Chem.* **2014**, *22*, 6638–6646.
- (46) Pine, S. H.; Sanchez, B. L. Formic acid-formaldehyde methylation of amines. *J. Org. Chem.* **1971**, *36*, 829–832.
- (47) Gawaskar, S.; Schepmann, D.; Bonifazi, A.; Robaa, D.; Sippl, W.; Wünsch, B. Benzo[7]annulene-based GluN2B selective NMDA receptor antagonists: Surprising effect of a nitro group in 2-position. *Bioorg. Med. Chem. Lett.* **2015**, *25*, 5748–5751.
- (48) Gawaskar, S.; Temme, L.; Schreiber, J. A.; Schepmann, D.; Bonifazi, A.; Robaa, D.; Sippl, W.; Strutz-Seeböhm, N.; Seeböhm, G.; Wunsch, B. Design, Synthesis, Pharmacological Evaluation and Docking Studies of GluN2B-Selective NMDA Receptor Antagonists with a Benzo[7]annulen-7-amine Scaffold. *ChemMedChem* **2017**, *12*, 1212–1222.
- (49) Ishiyama, T.; Murata, M.; Miyaura, N. Palladium(0)-Catalyzed Cross-Coupling Reaction of Alkoxydiboron with Haloarenes: A Direct Procedure for Arylboronic Esters. *J. Org. Chem.* **1995**, *60*, 7508–7510.
- (50) Wang, L.; Jacobson, O.; Avdic, D.; Rotstein, B. H.; Weiss, I. D.; Collier, L.; Chen, X.; Vasdev, N.; Liang, S. H. Ortho-Stabilized (18) F-Azido Click Agents and their Application in PET Imaging with Single-Stranded DNA Aptamers. *Angew. Chem., Int. Ed.* **2015**, *54*, 12777–12781.
- (51) Pajouhesh, H.; Lenz, G. R. Medicinal chemical properties of successful central nervous system drugs. *NeuroRx* **2005**, *2*, 541–553.
- (52) Szermerski, M.; Borgel, F.; Schepmann, D.; Haider, A.; Betzel, T.; Ametamey, S. M.; Wunsch, B. Fluorinated GluN2B Receptor Antagonists with a 3-Benzazepine Scaffold Designed for PET Studies. *ChemMedChem* **2018**, *13*, 1058–1068.
- (53) Preshlock, S.; Calderwood, S.; Verhoog, S.; Tredwell, M.; Huiban, M.; Hienzsch, A.; Gruber, S.; Wilson, T. C.; Taylor, N. J.; Cailly, T.; Schedler, M.; Collier, T. L.; Passchier, J.; Smits, R.; Mollitor, J.; Hoepfing, A.; Mueller, M.; Genicot, C.; Mercier, J.; Gouverneur, V. Enhanced copper-mediated (18)F-fluorination of aryl boronic esters provides eight radiotracers for PET applications. *Chem. Commun.* **2016**, *52*, 8361–8364.
- (54) Chenard, B. L.; Bordner, J.; Butler, T. W.; Chambers, L. K.; Collins, M. A.; De Costa, D. L.; Ducat, M. F.; Dumont, M. L.; Fox, C. B. (1S,2S)-1-(4-hydroxyphenyl)-2-(4-hydroxy-4-phenylpiperidino)-1-propanol: a potent new neuroprotectant which blocks N-methyl-D-aspartate responses. *J. Med. Chem.* **1995**, *38*, 3138–3145.
- (55) Bullock, M. R.; Merchant, R. E.; Carmack, C. A.; Doppenberg, E.; Shah, A. K.; Wilner, K. D.; Ko, G.; Williams, S. A. An open-label study of CP-101,606 in subjects with a severe traumatic head injury or spontaneous intracerebral hemorrhage. *Ann. N. Y. Acad. Sci.* **1999**, *890*, 51–58.
- (56) Preskorn, S. H.; Baker, B.; Kolluri, S.; Menniti, F. S.; Krams, M.; Landen, J. W. An innovative design to establish proof of concept of the antidepressant effects of the NR2B subunit selective N-methyl-D-aspartate antagonist, CP-101,606, in patients with treatment-refractory major depressive disorder. *J. Clin. Psychopharmacol.* **2008**, *28*, 631–637.
- (57) Schepmann, D.; Frehland, B.; Lehmkuhl, K.; Tewes, B.; Wunsch, B. Development of a selective competitive receptor binding assay for the determination of the affinity to NR2B containing NMDA receptors. *J. Pharm. Biomed. Anal.* **2010**, *53*, 603–608.
- (58) Meyer, C.; Neue, B.; Schepmann, D.; Yanagisawa, S.; Yamaguchi, J.; Wurthwein, E. U.; Itami, K.; Wunsch, B. Improvement of sigma1 receptor affinity by late-stage C-H-bond arylation of spirocyclic lactones. *Bioorg. Med. Chem.* **2013**, *21*, 1844–1856.
- (59) Miyata, K.; Schepmann, D.; Wünsch, B. Synthesis and σ receptor affinity of regioisomeric spirocyclic fuopyridines. *Eur. J. Med. Chem.* **2014**, *83*, 709–716.
- (60) Hasebein, P.; Frehland, B.; Lehmkuhl, K.; Fröhlich, R.; Schepmann, D.; Wunsch, B. Synthesis and pharmacological evaluation of like- and unlike-configured tetrahydro-2-benzazepines with the alpha-substituted benzyl moiety in the 5-position. *Org. Biomol. Chem.* **2014**, *12*, 5407–5426.
- (61) Chu, U. B.; Ruoho, A. E. Sigma Receptor Binding Assays. *Curr. Protoc. Pharmacol.* **2015**, *71*, 1.34.1–1.34.21.
- (62) Baumann, C. A.; Mu, L.; Johannsen, S.; Honer, M.; Schubiger, P. A.; Ametamey, S. M. Structure–Activity Relationships of Fluorinated (E)-3-((6-Methylpyridin-2-yl)ethynyl)cyclohex-2-enone-O-methyloxime (ABP688) Derivatives and the Discovery of a High Affinity Analogue as a Potential Candidate for Imaging Metabotropic Glutamate Receptors Subtype 5 (mGluR5) with Positron Emission Tomography (PET). *J. Med. Chem.* **2010**, *53*, 4009–4017.
- (63) Garner, R.; Gopalakrishnan, S.; McCauley, J. A.; Bednar, R. A.; Gaul, S. L.; Mosser, S. D.; Kiss, L.; Lynch, J. J.; Patel, S.; Fandozzi, C.; Lagrutta, A.; Briscoe, R.; Liverton, N. J.; Paterson, B. M.; Vornov, J. J.; Mazhari, R. Preclinical pharmacology and pharmacokinetics of CERC-301, a GluN2B-selective N-methyl-D-aspartate receptor antagonist. *Pharmacol. Res. Perspect.* **2015**, *3*, No. e00198.
- (64) Matsuno, K.; Nakazawa, M.; Okamoto, K.; Kawashima, Y.; Mita, S. Binding properties of SA4503, a novel and selective sigma 1 receptor agonist. *Eur. J. Pharmacol.* **1996**, *306*, 271–279.
- (65) Fischer, S.; Wiese, C.; Maestrup, E. G.; Hiller, A.; Deuther-Conrad, W.; Scheunemann, M.; Schepmann, D.; Steinbach, J.; Wunsch, B.; Brust, P. Molecular imaging of sigma receptors: synthesis and evaluation of the potent sigma1 selective radioligand [18F]-fluspidine. *Eur. J. Nucl. Med. Mol. Imaging* **2011**, *38*, 540–551.
- (66) Abate, C.; Ferorelli, S.; Contino, M.; Marottoli, R.; Colabufo, N. A.; Perrone, R.; Berardi, F. Arylamides hybrids of two high-affinity sigma2 receptor ligands as tools for the development of PET radiotracers. *Eur. J. Med. Chem.* **2011**, *46*, 4733–4741.